Aalto University
School of Chemical
Engineering

Keivan Khademi Kalantari

Fundamental understanding of nanocellulose– lignin interactions using mechano-enzymatically produced cellulose nanofibrils

Master's Programme in Life Science Technologies

Major in Biosystems and Biomaterials

Master's thesis for the degree of Master of Science in Technology submitted for inspection, Espoo, 14th of May, 2019.

Supervisor: Monika Österberg, Professor

Thesis instructor: Mika Sipponen, D.Sc. (Tech.)

Aalto University
School of Chemical
Engineering

Aalto University, P.O. BOX 11000, 00076 AALTO
www.aalto.fi

Abstract of master's thesis

Author Keivan Khademi Kalantari

Title of thesis Fundamental understanding of nanocellulose–lignin interactions using mechano-enzymatically produced cellulose nanofibrils

Degree Programme Life Science Technologies

Major Biosystems and Biomaterials

Thesis supervisor Monika Österberg

Thesis advisor Mika Sipponen

Date 14.05.2019 **Number of pages** 81 **Language** English

Abstract

Recently the development of wood-based materials has been a trending topic due to raised environmental consciousness. This new way of thinking has opened new markets and competition towards finding environmentally friendly alternatives to petroleum based products. VTT has developed a high consistency and simple method to produce cellulose nanofibrils (CNF) referred to as "HefCel", which is based on enzyme-assisted mechanical production of nanofibrillar cellulose. Herein HefCel and its interaction with colloidal lignin particles (CLPs) was studied by preparing nanocomposite films in order to obtain enhanced fundamental knowledge of their compatibility. Two different film preparation methods were applied in order to distinguish whether the production technique has an effect on the properties of the nanocomposite films. Moreover, treatment of the films with the enzyme laccase was used in an attempt to form crosslinks between lignin constituents and to evaluate possible changes in film properties. Produced nanocomposite films were characterized by electron microscopy (SEM, TEM), dry and wet tensile testing, and water contact angle (WCA) measurements. It was discovered that the preparation method had an influence on the properties of the nanocomposite films. Tensile stress at break and WCA values between ambient dried and filtered nanocomposite films ranged between ca. 19–56 MPa and 27–58°, respectively. Ambient dried nanocomposite films exhibited higher tensile properties compared to filtered nanocomposite films. Moreover, the ambient dried films showed generally higher WCA values exhibiting also stronger correlation to the lignin content compared to those of the nanocomposite films prepared with the filtration method. Finally, laccase experiment did not have a significant effect on tensile properties, however higher WCA values were discovered.

Keywords nanocellulose, CNF, HefCel, lignin nanoparticle, colloidal lignin particles, CLP, residual lignin, nanocomposite

Aalto-yliopisto
Kemian tekniikan
korkeakoulu

Aalto-yliopisto, PL 11000, 00076 AALTO
www.aalto.fi

Diplomityön tiivistelmä

Tekijä Keivan Khademi Kalantari

Työn nimi Nanoselluloosan ja –ligniinin välisten vuorovaikutusten tutkiminen hyödyntäen mekaanis-entsymaattisesti tuotettuja selluloosananofibrillejä

Koulutusohjelma Life Science Technologies

Pääaine Biosysteemit ja biomateriaalit

Työn valvoja Monika Österberg

Työn ohjaaja Mika Sipponen

Päivämäärä 14.05.2019 **Sivumäärä** 81 **Kieli** englanti

Tiivistelmä

Puupohjaiset materiaalit ovat saaneet viime aikoina paljon huomiota ympäristöystävällisinä vaihtoehtoina öljypohjaisten materiaalien korvaamiseksi. Tämän tutkimuksen tavoitteena oli saada perusteellista ymmärrystä VTT:n kehittämän entsyymiavusteisesti tuotetun nanoselluloosan (HefCel) ja kolloidisten ligniinipartikkelien välisistä vuorovaikutuksista valmistamalla ohuita nanokomposiittifilmejä paineistetulla suodatuksella ja valumenetelmällä, jossa veden annettiin haihtua normaaliolosuhteissa. Työssä tutkittiin myös erilaisten valmistusmenetelmien vaikutusta nanofilmien ominaisuuksiin. Lisäksi tutkittiin, vaikuttaako jäännösligniiniä sisältävien HefCel-filmien käsittely lakkaasi-entsyymillä filmien ominaisuuksiin. Nanokomposiittifilmejä karakterisoitiin elektronimikroskopiamenetelmillä (SEM, TEM), vetolujuusmittauksilla sekä mittaamalla veden kontaktikulma filmien pinnalla. Tulokset osoittivat valmistusmenetelmien vaikuttavan nanokomposiittien ominaisuuksiin. Vetolujuusarvot vaihtelivat 19–56 MPa, kun taas vesikontaktikulmat vaihtelivat 27–58^{o} valmistusmenetelmästä riippuen. Valumenetelmällä valmistettujen filmien vetolujuus- ja vesikontaktikulmalukemat olivat yleisesti korkeammat verrattuna suodatusmenetelmällä valmistettujen filmien arvoihin. Lakkaasikäsittely johti korkeampiin filmien kontaktikulma-arvoihin, mutta lujuusominaisuuksiin sillä ei ollut merkittävää vaikutusta.

Avainsanat nanoselluloosa, SNF, HefCel, ligniininanopartikkelit, kolloidiset ligniinipartikkelit, CLP, jäännösligniini, nanokomposiitti

Preface

First of all, I wish to express my sincere gratitude and appreciation to my supervisor Monika Österberg, for giving me the opportunity to be part of an interesting and important topic through this master's thesis. I would also like to thank my instructor Mika Sipponen for his exceptional guidance throughout this process and sending motivation all the way from Cuba – Thank you for encouragements and support during the days that I was not sure if I could make it. I also like to thank Farooq Mohammad for his help with the experimental part and Piritta Niemi, Jaakko Pere, and Stina Grönqvist for their collaboration. This project has taught me a lot, which has also given me a new perspective and inspired me on choosing my everyday path towards more sustainable lifestyle.

Finally my family and friends. First, I would like to thank my girlfriend Elina and her family for their support – Thank you for believing in me. Sakke and his family for giving me a roof over my head (which includes movie theatre and other goods, naturally of course). Susa and her family for letting this kid into your home and giving him the feeling of belonging. I would like to thank my uncle "daii" for being always there for me and my brother, supporting us in every way possible. My brother, thank you for affecting enthusiasm towards new things and setting up a good example for me every day - I'm proud of you. Ever since when my brother and I was born, my parents have done everything so we wouldn't feel left out. Thus, I would like to thank my mom "maman" for her love and strength throughout these years – I'm proud of you. My dad "baba", for not only being a supporting father but also excellent teacher – I know you are watching – This is for you.

Thank you.

This work was a part of the Academy of Finland's Flagship Programme under Projects No. 318890 and 318891 (Competence Center for Materials Bioeconomy, FinnCERES).

List of abbreviations

BC	Bacterial cellulose
CLPs	Colloidal lignin particles
CNCs	Cellulose nanocrystals
CNF	Cellulose nanofibrils
DLS	Dynamic light scattering
SEM	Scanning electron microscopy
TEM	Transmission electron microscopy

Table of Contents

LITERATURE REVIEW

1. Introduction

Every year enormous amount of harmful plastic waste is produced, which has brought many scientist together to solve this accumulating problem by finding better and more sustainable alternatives to petroleum-based materials. Lignocellulose components, the main components of plants, have gained a lot of attention lately, due to their vast potential as environmentally friendly materials. Cellulose nanofibrils (CNF) has a high promise to become a future high-performance material. CNF is not only renewable, it is also abundantly available, biocompatible, thermally stable, hydrophilic, possess high specific strength, and it is flexible to many chemical modifications (Österberg *et al.*, 2013). Lignin is another lignocellulose component, which has been long undervalued and utilized mostly as an energy source in pulp- and paper-making industry. However, lately lignin has gained much more respect and considered to have a lot of potential in more advanced applications (Kai *et al.*, 2016).

The focus of this Master's thesis was to gain fundamental understanding of the nature and interaction of CNF, which was produced using HefCel technology, and colloidal lignin particles (CLPs), which were prepared from softwood kraft lignin. The thesis consist of a literature review and an experimental section. The literature part reviews the relevant components of lignocellulose, their properties and common applications. The experimental study focused on the preparation of thin films of a new type of nanocellulose (HefCel) with CLPs to improve the understanding of interactions and properties of these two lignocellulose components, as well as their function and suitable properties towards new applications.

2. Plant-based biopolymers and their material properties

This chapter will give the reader an insight about the structure and properties regarding plant-based biopolymers in the following order: cellulose, hemicellulose, and lignin. However, cellulose and lignin are the most significant components for this thesis, thus they are described in more detail.

Wood is mostly comprised of cellulose, hemicellulose, and lignin. Additionally other substances can be found in lower quantities, such as pectin, starch, proteins, extractives, water-soluble organics, and inorganic compounds. The average chemical composition of Scots pine (softwood) and Silver birch (hardwood) is presented in **Figure 1**, showing that cellulose content is more or less the same, with 40% of dry solids. However, hemicellulose and lignin contents differ between softwood and hardwood, hardwood usually contains more hemicellulose and less lignin. According to Stenius (2000), Scots pine and Silver birch contain 25%-30% and 30%-35% hemicellulose, while the lignin content is 25%-30% and 20%-25% on dry basis, respectively. Moreover, both Scots pine and Silver birch contains around 5% of other compounds (mainly extractives) (Stenius, 2000).

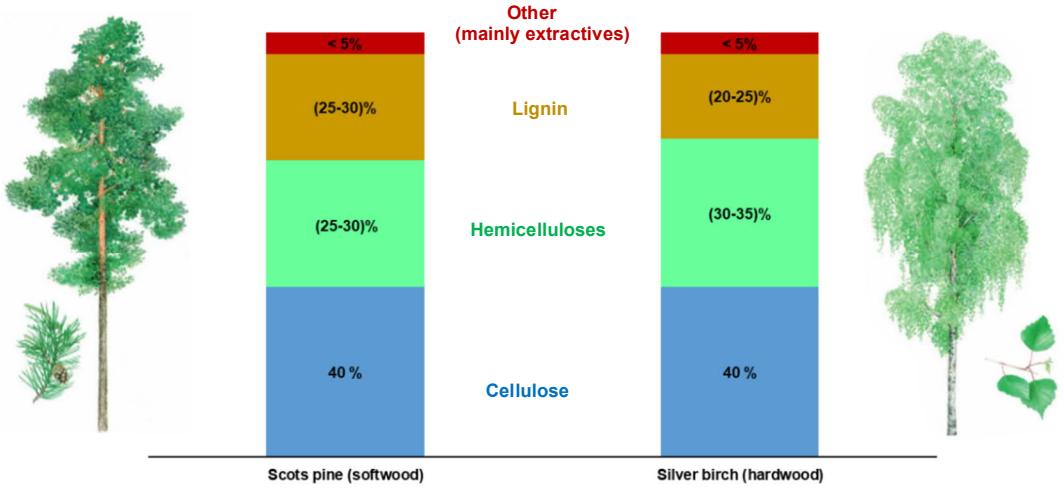

Figure 1. Chemical composition of softwood Scots pine (Pinus sylvesteris) and hardwood Silver birch (Betula pendula). Modified from Stenius (2000) and UPM The Biofore Company (2011). (Stenius, 2000; UPM, 2011)

The hierarchical structure of the cellulose biopolymer can be viewed from meter-to-nanometer scale, i.e., from the trunk of wood to molecular structure of cellulose. As shown in **Figure 2**, the cellulose molecules self-assemble together in an organized matter first forming elementary fibrils, which will then bundle up together forming cellulose microfibrils (CMF). The fibril structure also shows the crystalline and amorphous regions, which is a very debatable subject discussed more in **chapter 2.1**.

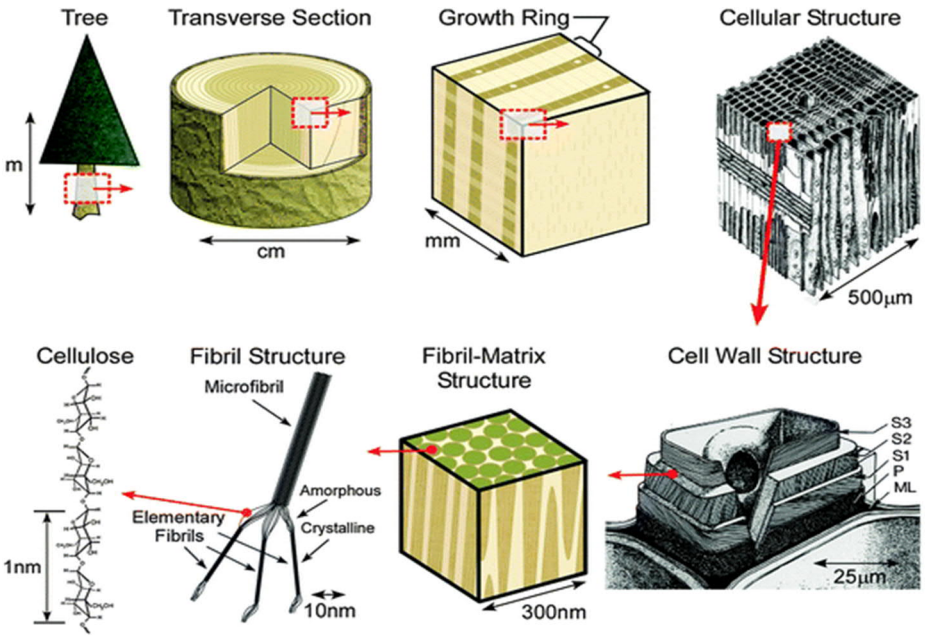

Figure 2. Schematic illustration of hierarchical structure of cellulose from tree to cellulose polymer structure. ML = Middle lamella, P = Primary cell wall, S1, S2, S2 = layers of cell wall (Moon *et al.*, 2011).

There has been a variety of models in attempt to explain the cellulose fibril structure and relationship with other wood constituents (hemicellulose, lignin). However, one of the widely accepted models shows that the elementary fibrils are surrounded by hemicellulose, which is further surrounded by lignin (**Figure 3**) (Fengel and Wegener, 1984).

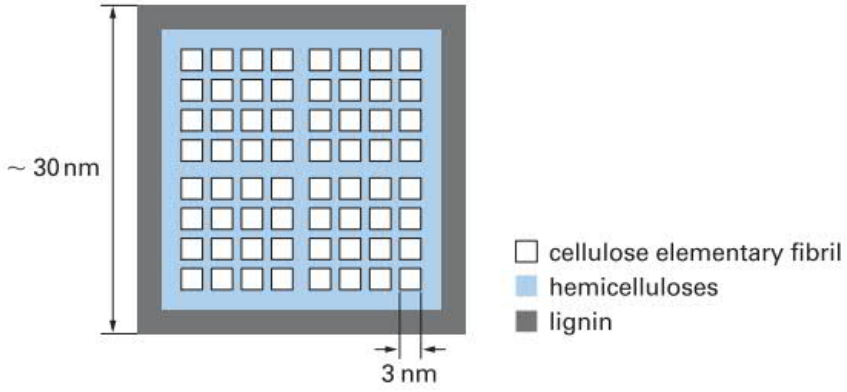

Figure 3. Model of fibril structure consisting of elementary fibrils, which are surrounded by hemicellulose and lignin (Fengel and Wegener, 1984).

Fengel's and Wegener's fibril structure model is quite simplified, however it does explain the composite nature and the interaction between the lignocellulose polymers. There has been many studies however, attempting to show the interactions between fibril constituents including lignin-carbohydrate complexes (LCC). Houtman and Atalla (1995) used molecular dynamics modelling in an attempt to explain the interactions between lignin and cellulose, showing that lignin precursor and lignin oligomers has a tendency to absorb on the surface of cellulose (Houtman and Atalla, 1995). Besides lignin-cellulose interactions, Hayashi, Marsden and Delmer (1987) studied the interaction between hemicellulolose (xyloglucan) and cellulose fibrils, suggesting that the association between them is source dependent and very specific (Hayashi, Marsden and Delmer, 1987). Moreover, Nishimura et al. (2018) were able to show the existence LCCs in which lignin forms covalent bonds with plant cell-wall carbohydrates. **Figure 4** is an illustration of hierarchical structure of lignocellulose biopolymers derived from a tree, further showing the linkages between lignin and hemicellulose (Nishimura *et al.*, 2018).

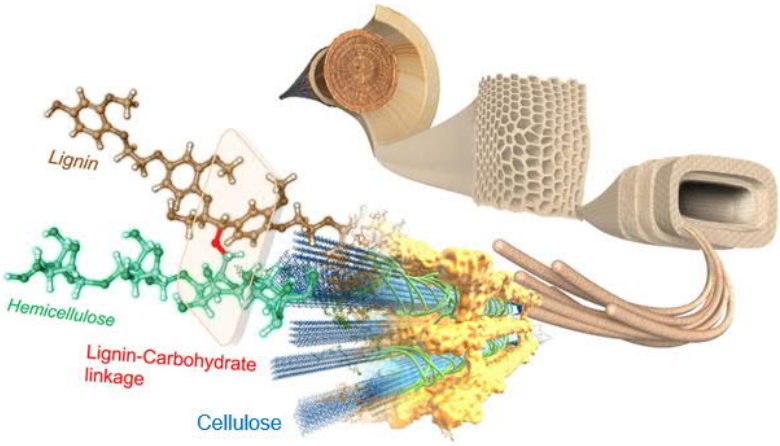

Figure 4. Schematic model of the hierarchical structure of lignocellulose components, showing the covalent bonding between lignin and hemicellulose also called lignin-carbohydrate complex (LCC). Modified from Nishimura et al (2018).

Ilyama et al. (1994) presented different variety of possible lignin-carbohydrate (LC) linkages in **Figure 5** including e.g., different ether and ester linkages. As reviewed, in a study by Sipponen et al. (2017) many of these LC linkages have been confirmed in recent years by using nuclear magnetic resonance (NMR) spectroscopy (Sipponen, Rahikainen, *et al.*, 2017). Although most of these so-called lignin carbohydrate complexes (LCCs) incorporate hemicelluloses and lignin, also cellulose-based LCCs have been evaluated (Lawoko and Henriksson, 2005).

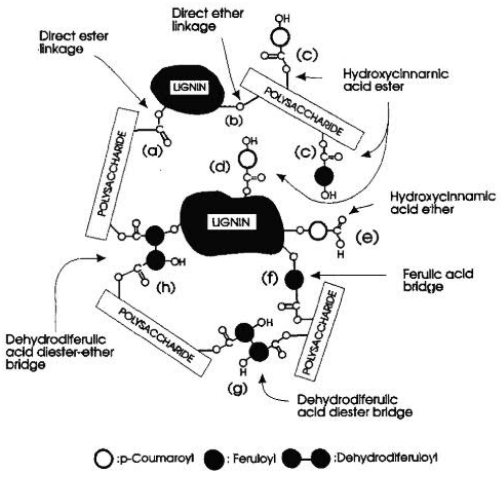

Figure 5. Possible covalent lignin-carbohydrate linkages in plant cell wall (Iiyama, Lam and Stone, 1994).

The lignocellulosic constituents are discussed in more detail in the next chapter starting from cellulose and then moving on to hemicelluloses and finally lignin.

2.1. Cellulose

Cellulose is the most abundant polysaccharide found in nature, and to give a good perspective it is estimated that more than 10^{12} tons of cellulose is naturally synthesized every year (Klemm *et al.*, 2005). There are many sources for cellulose such as certain species of bacteria (*gluconacetobacteria xylinum*), tunicates (*animal cellulose*), and plants. This thesis however concentrates mostly on plant-derived cellulose, which is also the most abundant source compared to the other sources mentioned. (Börjesson and Westman, 2015)

Cellulose is an organic polymer, which consists of D-anhydroglucopyranose units (AGU) linked via β-1,4-glycosidic bonds into a linear homopolymer chain. There are three different AGU units: reducing end group containing either hemiacetal or aldehyde group at the C1 (first carbon) position, non-reducing end group that has a free hydroxyl group at the C4 position, and also internal anhydroglucose rings that connect the reducing and non-reducing ends at the C1 and C4 positions (**Figure 6**) (Eyley and Thielemans, 2014).

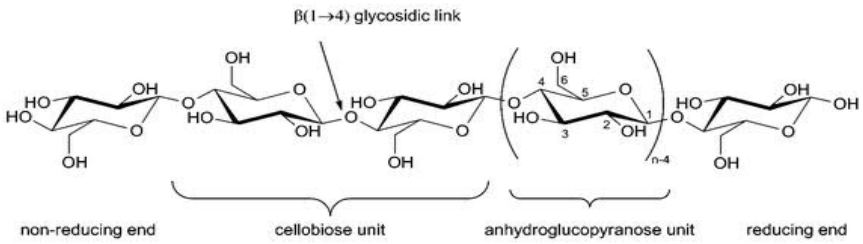

Figure 6. The molecular structure of cellulose consisting of cellobiose 1,4-β-D-glucopyranose, which is the smallest repeating unit forming a long homopolymer (Eyley and Thielemans, 2014).

Degree of polarization (DP) is used to describe the length of the polymer. It determines the amount of monomeric units within the polymer, thus in case of cellulose the amount of anhydroglucose units. The length or the DP value in cellulose however varies depending on the source and treatment *i.e.* cellulose from plant source can reach the DP value of 13000-14000 whereas bacterial cellulose and cotton based cellulose DP value can vary between 2000-6000 (Jonas and Farah, 1998). (Klemm *et al.*, 2005)

Cellulose fibers, rich in hydroxyl groups, can form inter- or intramolecular hydrogen bonds **(Figure 7**). Intramolecular hydrogen bonds exist between the hydroxyl groups within the cellulose chain, which provides stiffness to the structure. Intermolecular hydrogen bonds are interactions between two adjacent polymers, which are also responsible for constructing sheet structures between individual units (Börjesson and Westman, 2015). It is also worth noting that the hydroxyl groups play an important part in chemical interactions, especially the free hydroxyl group at the C-6 position, which is also the most reactive and enables chemical modification for various functionalities (Roy *et al.*, 2009).

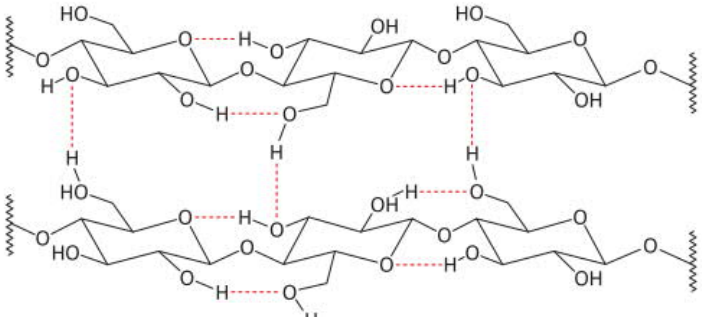

Figure 7. Schematic image of inter- and intramolecular bonds in cellulose molecule (Dufresne, 2012).

For long, there has been uncertainty about the structure of cellulose microfibrils (CMF). That said, a common structural model of CMF is the fringed-fibrillar model,

which consist of highly organized crystalline regions and irregular interruptions also referred to as “amorphous” regions **(Figure 8)**. The crystalline structure is due to the intermolecular bonds mentioned earlier between different cellulose biopolymers, which are aligned together in a parallel direction.

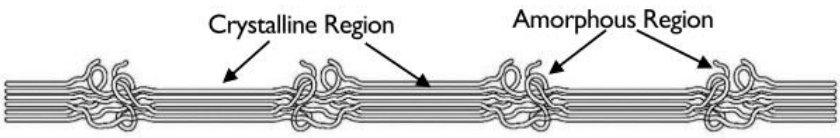

Figure 8. Illustration of fringed-fibrillar model showing the crystalline and amorphous regions within CMF (J.L., Bédué and Mercier, 2010).

However, Nishiyama et al. (2003) challenged this conventional view of fringed-fibrillar model using small angle neutron scattering (SANS) technique. In their study, they found out that the irregular and bulky so called “amorphous” regions, which are typical for synthetic polymer (J. Loos, P. C. Thüne, J. W. Niemantsverdriet, 1999), are in fact just a defects of a few anhydroglucose units. (Nishiyama *et al.*, 2003) That said, the term “amorphous” will be used in this Thesis referring however to the defect zones in the crystalline structure **(Figure 9)**.

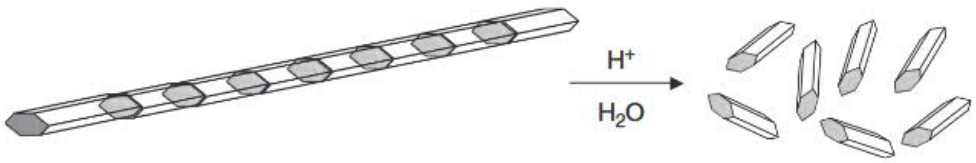

Figure 9. Acid hydrolysis of cellulose microfibrils (Rosenau, Antje and Hell, 2019).

In the following chapter the production, properties, and applications of nanocellulose is described in more detail.

2.2. Hemicelluloses

Hemicelluloses are heteropolysaccharides located in plant cell walls. They are composed of β-(1→4)-linked backbones with an equatorial configuration. Their natural function is to strengthen the cell walls by interacting with cellulose, and in some cases with lignin (Scheller and Ulvskov, 2010). The complex and multifold nature of hemicellulose has raised discussions on how to group them, however this thesis will use the grouping method, which is widely used by Scheller and Ulskov (2010), and many other workers in this field. The hemicelluloses can be divided to xyloglucan, xylans, mannans, glucomannans, and β-(1→3,1→4)-glucans **(Figure 10)**. This definition method is based on the similar backbone structure having β-(1→4) linkage to either glucose, mannose, or xylose. (Scheller and Ulvskov, 2010)

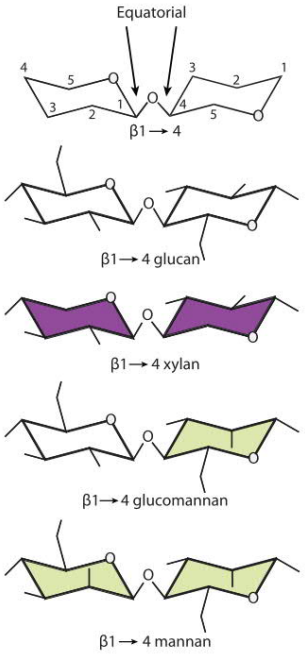

Figure 10. Hemicelluloses (Scheller and Ulvskov, 2010).

Hemicelluloses are widely utilized in food and feed industry (Scheller and Ulvskov, 2010), but other applications has also been reported. E.g. Lian et al. (2018) used hemicellulose based hydrogel in attempt to absorb heavy metal ions (Lian *et al.*, 2018)

2.3. Lignin

In this chapter the chemical structure, different extraction methods of lignin and commercialized products are described. The kraft lignin extraction process is described more in detail, since kraft lignin was selected for the experimental part of this master's thesis.

Lignin is the second most abundant biopolymer from biomass after cellulose. According to Smolarski (2012) the availability of lignin comprises more than 300 billion tons annually and increasing every year by 20 billion tons (Smolarski, 2012). (Laurichesse and Avérous, 2014). The natural role of lignin in botanical environment is providing strength and structure to the cell walls, controlling the water permeation and transport, and protecting the plant from enzymatic degradation of other components in wood structure (Boerjan, Ralph and Baucher, 2003). The paper and pulp industry have considered lignin mostly as a waste byproduct, which has been utilized as an energy source for running the paper mills. According to Laurichesse and Avérous (2014), 50 million ton of lignin has been extracted during 2010, but only 2 % has been utilized for further applications. However, more recently, lignin has started to receive more attention for its potential for more advanced applications and due to increased production rate of cellulose pulp fibers, thus increasing the availability of lignin (Bruijnincx, Rinaldi and Weckhuysen, 2015; Kai *et al.*, 2016). **Table 1** presents proposed potential applications and already commercialized products of lignin. Due to water solubility and high average molar-mass, Lignosulfonate lignin are well utilized as industrial additives, binders, dispersants, and surfactants. Moreover, kraft lignin has been considered for high performance material as a carbon fiber production.

Table 1. Commercialized Lignin products and potential applications.

Commercialized products	Reference
Binder	(Laurichesse and Avérous, 2014)
Additive	
Surfactant	
Dispersant	
Potential applications	**Reference**
Carbon fiber	(Gellerstedt, 2015)
Wood adhesive	(Silva *et al.*, 2013)
Feed additive (possible antimicrobial activity)	(Baurhoo, Ruiz-feria and Zhao, 2008)

Lignin is an amorphous heteropolymer comprising of phenylpropane units (Sarkanen and Ludwig, 1971; Stenius, 2000), which are the products of lignification reaction between three different aromatic alcohols or monolignols: p-coumaryl alcohol, coniferyl alcohol, and sinapyl alcohol (Dorrestijn *et al.*, 2000). These phenolic alcohols form the corresponding structural units called p-hydroxyphenol (H), guaiacyl (G), and syringyl (S) units respectively (**Figure 11)** (Laurichesse and Avérous, 2014).

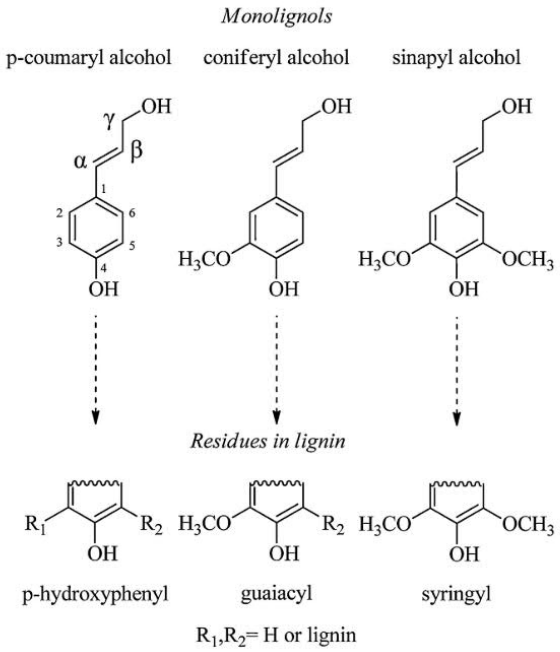

Figure 11. Monolignols (precursor of lignin) and their corresponding structures (Laurichesse and Avérous, 2014).

Lignification process is an enzymatic dehydrogenative polymerization reaction between monolignols, which comprises of various oxidative coupling reactions. According to Vanholme et al. (2010) the polymerization reaction is catalyzed by laccase and/or peroxidase enzymes where the former uses oxygen, whereas the latter mentioned uses hydrogen peroxide as co-substrate to oxidize their metal center in order to perform catalytical phenol oxidation. Another component in the lignin polymerization reaction is the formation of quinone methides, which are an initial products during radical coupling of monolignols. (Ralph *et al.*, 2009; Vanholme *et al.*, 2010) **Figure 12** exhibits an example of monolignols being oxidized into various radicalized quinone methides.

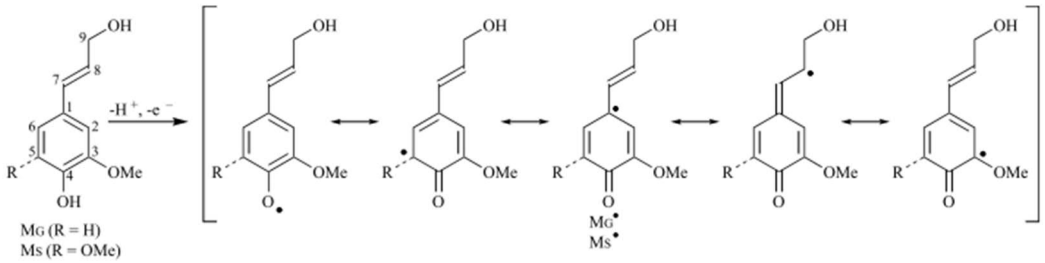

Figure 12. Radical delocalization after single electron subtraction from coniferyl alcohol (MG) or sinapyl alcohol (MS) (Ralph et al., 2009).

The phenylpropane units are connected by ether linkages (C-O-C) and carbon-carbon bonds (C-C), however the former ones are more frequent due to the abundant β-O-4 bonds that comprise more than half of all inter unit linkages in native lignins (Adler, 1977; Dimmel, 2010). The most usual linkages for softwood lignin are depicted in **Figure 13** including α-O-4, 5-5, β-β, α-O-5, β-5, β-1 (Stenius, 2000; Laurichesse and Avérous, 2014)

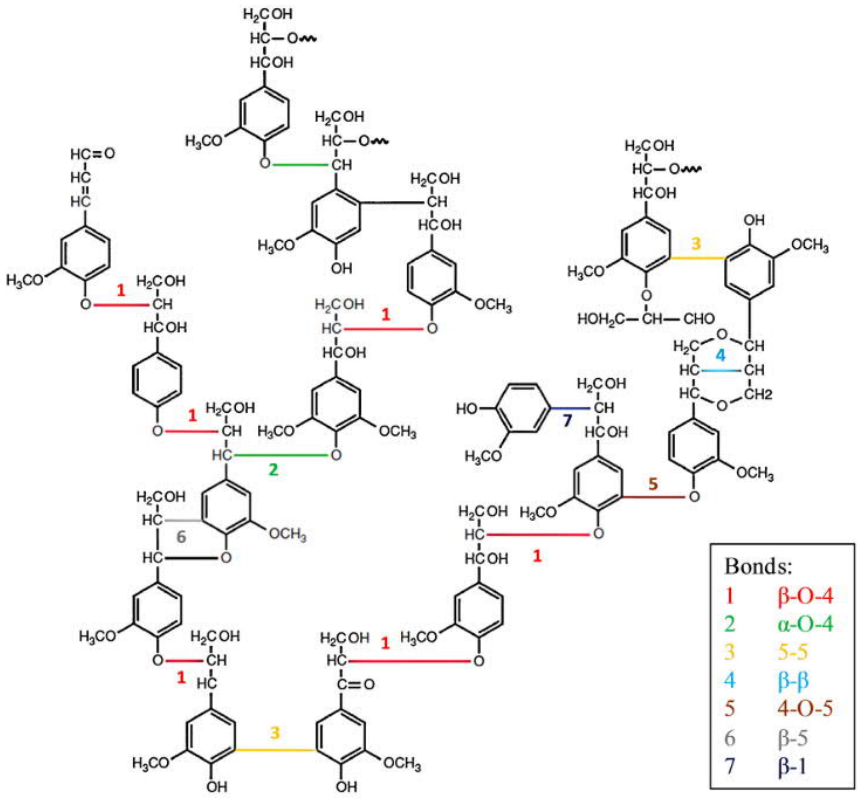

Figure 13. Typical linkages in softwood lignin (Laurichesse and Avérous, 2014).

Lignins are categorized into three main groups based on the native source: softwood lignins, hardwood lignins, and grass lignins. These lignin types are extracted from their respective sources in many forms such as “dioxane lignin”, “milled wood lignin” (MWL), or “enzymatically liberated lignin”. Furthermore, lignins are classified into several different technical lignins resulting from the different pulping processes presented in **Figure 14**. The lignin extraction may be done in two ways using sulfurous and sulfur-free process. The former produce lignosulfonate and kraft lignin whereas the sulfur-free processes result in organosolv and soda lignin. Although the vast majority of lignin produced in pulp and paper industry is utilized as an energy source within the process, modern pulping technology allows substantial recovery of lignin for other applications. (Stenius, 2000; Laurichesse and Avérous, 2014)

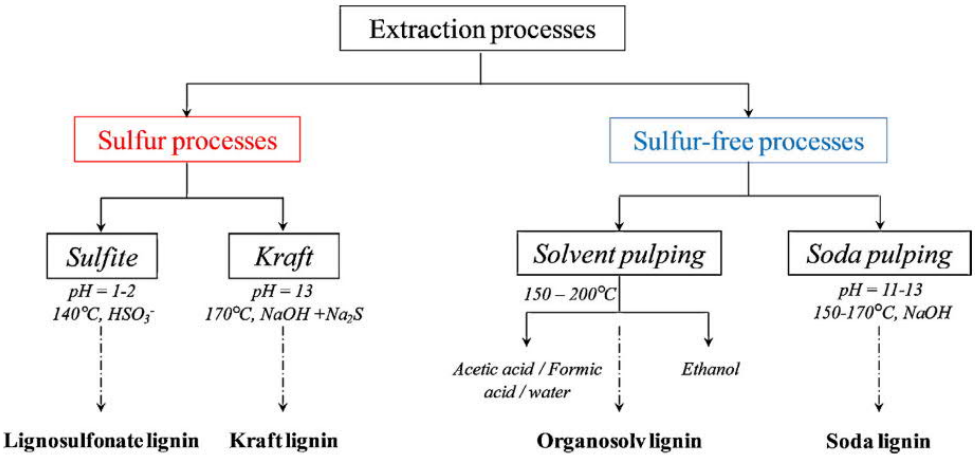

Figure 14. Schematic presentation of lignin extraction processes. (Laurichesse and Avérous, 2014)

There are several challenges in the attempt to utilize lignin. One of the limitation is its inaccurately defined and varying chemical structure, for it is very source dependent (Laurichesse and Avérous, 2014). Even though some hypothetical chemical formulas are widely presented, it is evident that the final form is a result of degradation during the lignin isolation process (Chakar and Ragauskas, 2004; Crestini *et al.*, 2017). Another limitation is the high variety in solubility of lignin. The kraft pulping is the most abundant industrial level chemical pulping process comprising three phases called "white liquor phase", "black liquor phase", and "green liquor phase" **(Figure 15).** The aim is to separate as much lignin as possible to reduce chemical consumption in the pulp bleaching phase. The degree of delignification and level of whiteness is tracked by the kappa number. The kraft pulping process starts with digesting the wood chips with white liquor containing sodium hydroxide (NaOH) and sodium sulfide (Na_2S) in aqueous solution. These chemicals extract lignin from wood, which will liberate the fibers and make the cooking liquor black.

The delignification process is highly influenced by the presence of HS^- due to its strong nucleophilicity, which will break aryl ether linkages and generate more free phenolic groups while increasing the hydrophilicity of lignin. Thus, lignin goes through a severe degradation phase. (Gellerstedt, 2015)

Next, lignin-containing black liquor (weak black liquor) is separated from the pulp fibers by washing and concentration using multiple-effect evaporators. Then, the concentrated black liquor (heavy black liquor) is combusted in a recovery boiler where energy is produced and the cooking chemicals are recovered.

Before achieving "white liquor phase" again, the combustion of the black liquor produces inorganic melt containing sodium carbonate (Na_2CO_3), sodium sulfide (Na_2S), and a small amount of sodium sulfate (Na_2SO_4), which are dissolved in water to form green liquor. During this "green liquor phase", NaOH is recovered by adding lime (CaO) to green liquor, thus regenerating the white liquor. (Stenius, 2000)

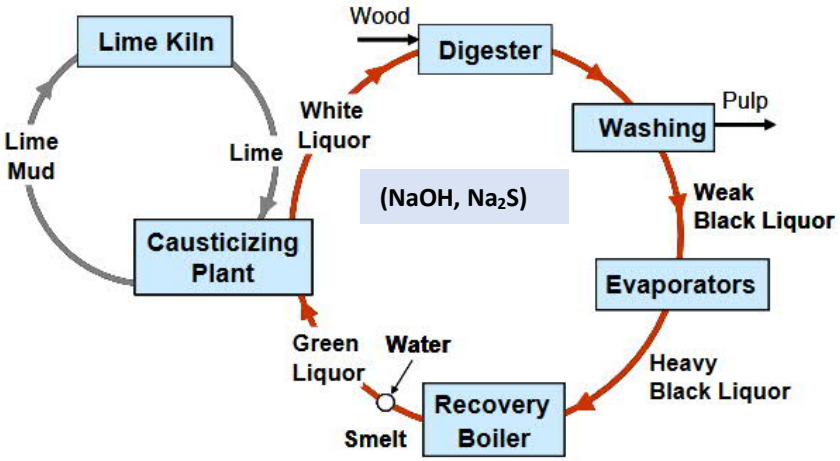

Figure 15. Kraft chemical recovery process. Modified from Vakkilainen and Tran, 2007.

Generally, lignin is precipitated by acidification followed by a sequence of filtration and washing (Stenius, 2000). Traditional lignin separation methods causes plugging of the filtration system, which will further cause problems; washing liquors cannot pass the lignin cakes properly, and high level of impurities in lignin will occur. These problems are due to changes in lignin solubility, which is further affected by the excessive pH levels and ionic strength gradient. LignoBoost process, developed by the

Swedish company Innventia and currently owned by the Finnish company Metso is a modern and patented method for lignin precipitation (**Figure 16**). The process consist of series of acidification, filtration and washing steps; the acids used in this process are CO_2 and H_2SO_4. With this process, clogging of the filters is avoided by re-dispersing the precipitated lignin and acidifying it further. Other stated advantages of the process are: low cost (acidic washing water, sulfuric acid, and filtration area can be kept low), high lignin yield, low ash and carbohydrate content, and high dry solid content. (Tomani, 2010)

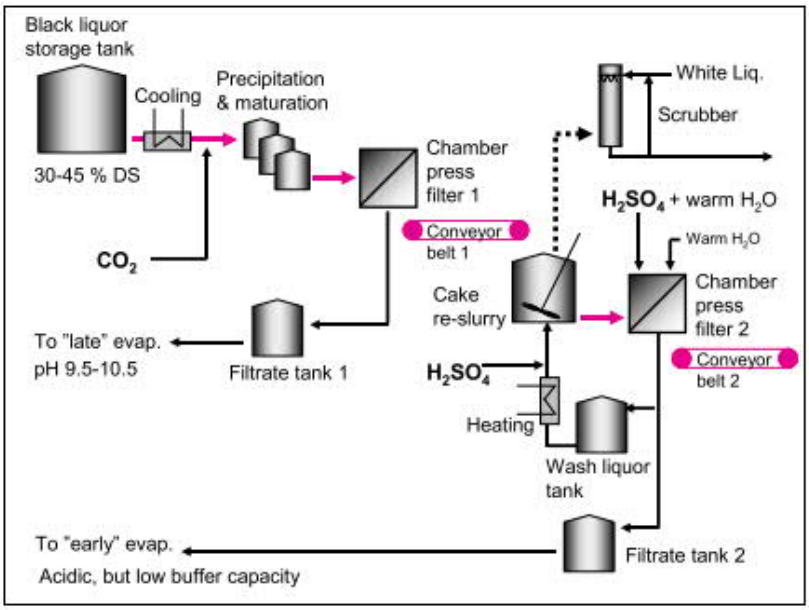

Figure 16. Schematic illustration of lignin separation from black liquor by Lignoboost process (Tomani, 2010).

3. Nanocellulose and lignin particles

3.1. Plant-based nanocellulose

This chapter covers the nanocellulose extraction methods, properties, and challenges. In addition, a technology called “high-consistency enzymatic fibrillation” (HefCel) is also described as it has a big role in this Master’s thesis. Nanocellulose is referred to in various different terms depending on the extraction method such as cellulose nanofibril (CNF) which is a product of mechanical shearing actions, chemically produced cellulose nanocrystal (CNC) which was first discovered by Rånby in 1949 in Sweden (Rånby, 1949), and finally bacterial cellulose (BC) which is produced by certain bacteria species (BC is discussed in more detail in chapter 3.2).

3.1.1. Cellulose nanofibrils

Mechanical extraction strategy consists mainly of high-pressure homogenization and may include grinding as well. During homogenization, the viscosity level of the suspension will rise making the structure more gel-like. Furthermore, homogenization and grinding procedures are very energy-consuming, therefore several pretreatment methods are suggested for more efficient fibril separation. To name a few, Herrick et al. (1983) used mechanical cutting, whereas Boldizar et al. (1987) utilized acid hydrolysis. In addition, Henrikson et al. (2007) and Pääkkö et al. (2007) used enzymes as a pretreatment procedure, whereas Wågberg et al. (2008) and Okita et al. (2011) introduced charged groups through carboxylation and 2,2,6,6-tetramethylpiperidine-1-oxyl (TEMPO) mediated oxidation, respectively. (Herrick *et al.*, 1983; Boldizar *et al.*, 1987; Henriksson *et al.*, 2007; Pääkkö *et al.*, 2007; Wågberg *et al.*, 2008; Okita *et al.*, 2011; Dufresne, 2012)

Figure 17 shows a photograph of CNF aqueous suspension with 2 wt% of dry weight after homogenization acquired from eucalyptus; however, there are also other sources of CNF. It is also worth noting that 2 wt% is an ideal suspension concentration, since larger concentration will cause viscosity level to rise too much. (Dufresne, 2013)

Figure 17. Mechanically extracted (enzymatically pretreated) 2 wt% CNF suspension obtained from eucalyptus (Lavoine *et al.*, 2012).

HefCel or high-consistency enzymatic fibrillation is a technology patented by VTT to prepare CNF mechanically in the presence of cellulase enzymes. **Figure 18** is a summary of the HefCel process, which begins with agitation of raw material at up to 40 % consistency in the presence of a tailored cellulase enzyme mixture. The enzyme activity and friction between cellulose fibers causes the formation of CNF. After CNF is acquired, the enzymes must be inactivated by increasing temperature, then washed and finally filtered. In the end of the process, the final product will be a paste-like material with 20-30% consistency of CNF, which is much higher than 1-3% of commonly obtained in the CNF production. (Kangas *et al.*, 2016)

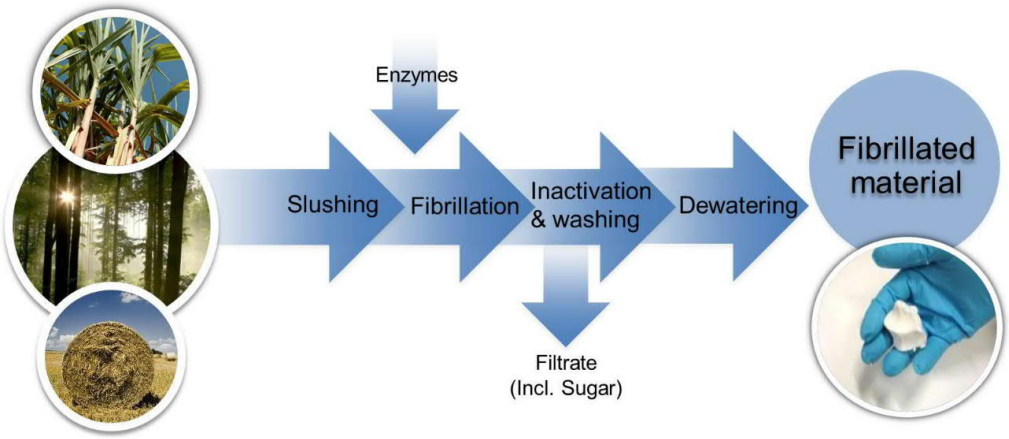

Figure 18. HefCel process. (Kangas *et al.*, 2016)

3.1.2. Cellulose nanocrystals

Chemically induced extraction process dissolves the amorphous regions (discontinuous defects in crystalline region) of the cellulose polymers using strong acid hydrolysis and further sonication treatment. This is in contrast with the mechanical preparation of CNF, where the amorphous and crystalline regions are still retained. Several different acids have been reported for the cellulose degradation process such as phosphoric acid (H_3PO_4), nitric acid (HNO_3), hydrobromic acid (HBr), sulfuric acid (H_2SO_4), and hydrochloric acid (HCl), sulfuric acid clearly being the most frequently used. (Dufresne, 2013)

The final shape after the chemical treatment is short needle shaped structures in aqueous environment called cellulose nanocrystals or nanowhiskers (CNCs). It has been observed that the whiskers possess birefringent domains when placed between crossed nicol prisms **(Figure 19)** (Siqueira and Abdillahi, 2010)**.** In addition to the more conventional acid hydrolysis, there are also other methods reported for preparing the CNCs. Siquiera et al. (2010) treated cellulose with enzymes (Siquieira *et al.*, 2010), whereas Man et al. (2011) used ionic liquid (Man *et al.*, 2011). Moreover Kontturi (2011) used gaseous acid for cellulose hydrolysis (Kontturi, 2011) whereas Hirota

(2010) applied TEMPO-mediated oxidation after acid hydrolysis (Hirota *et al.*, 2010). (Dufresne, 2013)

Figure 19. Capim dourado cellulose nanocrystals between cross-nicols showing the birefringent domains (left) and Transmission electron micrograph image of ramie nano crystals (Siqueira and Abdillahi, 2010).

Generally, microscopy techniques are used for evaluation of the morphology of the nanoparticles. **Figure 20** shows transmission electron microscopy (TEM) images of both CNF and CNCs. According to Klemm et al. 2011, the width and length of CNCs are 7-70 nm and from 100 nm to several micrometers, respectively (Klemm *et al.*, 2011). The length of the CNF is considered to be higher than 1 µm, in fact, according to Österberg et al. (2013), it may exceed 5 µm. However, it is hard to evaluate length since the fibrils are entangled to each other, whereas the width is more noticeable giving values in the range of 3-100 nm (Dufresne, 2012). The dimensions of nanocellulose depends on the source, defibrillation process, and pretreatment process. The lack of defect regions in CNC structure gives better mechanical property than mechanically extracted CNF, thus the longitudinal modulus is considered to be around 130 GPa and 100 GPa, respectively. That said, CNCs have more tendency to

form aggregates due to their smaller size and therefore larger specific surface area, which is further harder to manage *e.g.* during nanocomposite film preparation (Dufresne, 2013). According to Dufresne these aggregations caused by inter-particle interactions will cause the loss of the nanoscale and limit the potential of the impressive mechanical properties mentioned above.

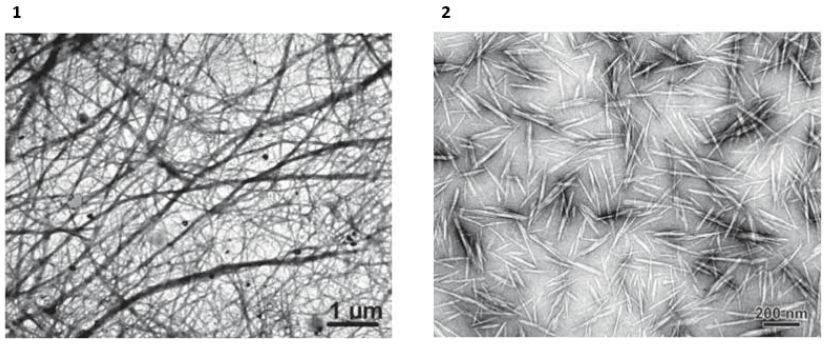

Figure 20. Transmission electron microscopy (TEM) image of 1. Cellulose nanofibrils (CNF) from Opuntia ficus-indica fibers (Malainine *et al.*, 2003) and 2. chemically treated CNC:s from ramie (Habibi *et al.*, 2008)

3.2. Bacterial cellulose

In addition to plant-based cellulose there are other cellulose sources, bacteria. Although bacterial cellulose (BC) is not the main topic for this thesis, it is still worth mentioning due to its unique structure and potential applications.

There are several bacteria reported to produce cellulose such as genera *Gluconacetobacter, Agrobacterium, Pseudomonas, Rhizobium, Sarcina* etc. However, according to Shoda and Sugano et al. (2005), *Gluconacetobacter xylinum* is the most advanced cellulose producing microorganism reported as of yet (Shoda and Sugano, 2005). (Jonas and Farah, 1998) Like plant-based cellulose, also bacterial cellulose is composed of β-1,4-linked anhydroglucose units, therefore they are chemically identical at the molecular level. In addition, BC has several similar characteristics with plant-derived cellulose e.g., biocompatibility and biodegradability. That said, there are many properties that make BC distinct from plant-based cellulose such as purity.

Unlike plant cellulose that is associated with hemicellulose and lignin, BC is excreted free in the extracellular matrix. However, BC has to be purified from the growth media and bacteria before use.(Klemm *et al.*, 2001; Shoda and Sugano, 2005) As mentioned in **Chapter 1**, the final BC could have DP value of 2000-6000 whereas the plant based cellulose have over 10 000 (Jonas and Farah, 1998). BC has larger specific surface area in contrast with plant based cellulose. The large surface area of BC is due to high aspect ratio of the fibers, which will give high liquid holding capacity to the structure (Sulaeva *et al.*, 2015).

The BC synthesis route is presented in **Figure 21** (Ul-islam, Khan and Khattak, 2015). The BC production goes through a complex, but precise pathway involving many different enzymes and regulators. The growing polymer extrudes through the cellulose export compounds, which are then self-assembled into microfibrils and further into bundles forming ribbons.

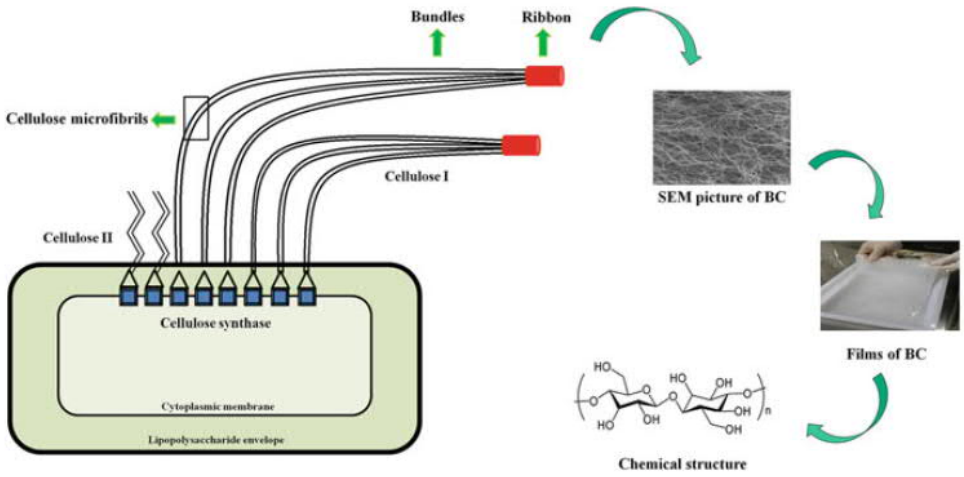

Figure 21. Schematic presentation of the hierarchichal structure and production of BC (Ul-islam, Khan and Khattak, 2015).

These material properties of bacterial cellulose are all valuable for further different medical applications, such as wound dressing applications, implants and drug delivery systems since the materials has to be mechanically stable, it has to have a

proper liquid absorption capacity, and living tissue does not create rejecting reactions.(Sulaeva *et al.*, 2015) However BC have many other applications in non-biomedical fields as well such as packaging, food, biosensors, paper, electronics etc. (Rajwade, Paknikar and Kumbhar, 2015).

3.3. Lignin nanoparticles

As mentioned before, a big setback for utilizing lignin has been its complex chemical structure and solubility. In addition, the insolubility of kraft lignin in water at neutral pH is also a major hindrance for industrial applications. However, recently developed colloidal lignin particles (CLPs) tackle this problem by creating aqueous dispersions of lignin nanoparticles (LNPs), which, although not dissolving lignin, will help lignin to disperse homogeneously in water. (Lievonen *et al.*, 2016)

Frangville et al. (2012) prepared irregular sizes and shapes of LNPs with wide range of pH stability (pH 1-9) by first dissolving low-sulfonate lignin in ethylene glycol which follows the precipitation using hydrochloric acid (HCl) (Frangville, 2012). Gilca et al. (2014) were able to prepare stable but irregular shaped LNPs by modifying lignin with ultrasonication (Gilca, Popa and Crestini, 2015), whereas Gongunta et al. (2012) used freeze-drying followed by thermal carbonization process to produce irregularly shaped lignin based carbon nanoparticles (Gonugunta *et al.*, 2012). Yiamsawas et al. (2014) synthesized hollow and irregularly shaped lignin based nanocapsules, which are consider to be useful in agricultural applications as nanocontainers (Yiamsawas *et al.*, 2014). Qian et al. (2014) managed to prepare pH-stable (<pH 12) spherical shaped LNPs from acetylated lignin in the presence of THF and water. (Qian, Deng, *et al.*, 2014). Lievonen et al. (2016) produced spherical colloidal lignin particles that were stable between pH 4-10 by one-step dialysis of lignin solution in THF against deionized water. These authors showed that acetylation of lignin was not required to achieve spherical lignin particles. Qian et al. (2014) also introduced a method to produce LNP functioning as a surfactant, which are CO_2 and N_2 responsive for Pickering emulsions (Qian, Zhang, *et al.*, 2014). Moreover, Ago et al. (2016) were able

to produce dry spherical lignin particles using an aerosol flow reactor (Ago *et al.*, 2016). The nanoparticles described above have been summarized in **Figure 22** for comparison.

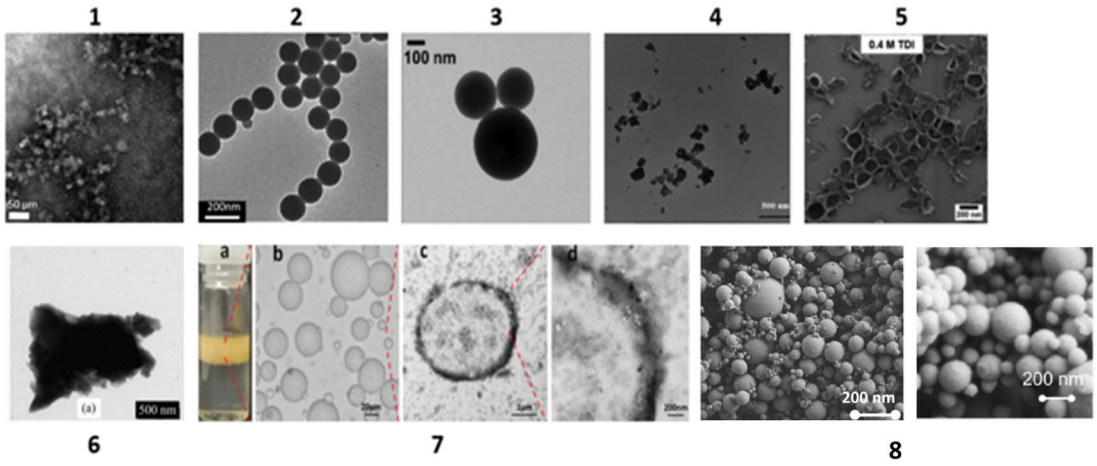

Figure 22. Lignin nanoparticle comparison between different methods. 1) Irregularly shaped LNPs. Modified from Frangville (2012) 2) Modified from Qian, Deng, et al. (2014) 3) Colloidal lignin particles. Modified from Lievonen et al. (2016) 4) Irregularly shaped LNPs. Modified from Gilca, Popa and Crestini (2015) 5) Irregularly shaped LNPs. Modified from Yiamsawas et al. (2014) 6) Irregularly shaped LNPs. Modified from Gonugunta et al. (2012) 7) CO_2 and N_2 responsive LNPs (Qian, Zhang, *et al.*, 2014) 8) Dry spherical lignin particles originated from Organosolv lignin (left) and Kraft lignin (right). Modified from Ago et al. (2016)

4. Applications of nanoscaled cellulose and lignin

Petroleum based products have been present in our everyday life for a long time due to their low production cost, simple processing, and superb technical properties. However, environmental concerns and limited availability of fossil recourses have awakened demand for more cost-efficient and sustainable alternatives. (Dufresne, 2012; Österberg *et al.*, 2013) Both nanocellulose and nanolignin have gained lot of attention due to their impressive properties and availability, which are considered a

valid solution for more sustainable industry. Herein, several applications reported in the literature has been presented.

Nanocellulose has many good qualities which makes it a good candidate for many applications. Non-toxic and biocompatible nature of cellulose has potential in pharmaceutical applications, whereas low thermal expansion coefficient, high aspect ratio, good mechanical and optical properties makes nanocellulose suitable material for e.g. paper making, coating additives, packaging, flexible screens etc. **Table 2** presents applications based on plant based nanocellulose found in the literature.

***Table 2**. Applications of plant based nanocellulose. Adapter from Sharma et al. 2019.* (Sharma *et al.*, 2019)

Category	Applications	Reference
Paper and Packaging	Intelligent packaging, UV screening packaging, antimicrobial packaging, transparent packaging	(Abdul Khalil, H.P.S. Davoudpour *et al.*, 2016; Boufi *et al.*, 2016; Osong, Norgren and Engstrand, 2016; Azeredo *et al.*, 2017)
Composites and plastics	Shelf life extension, Heat resistance, Dimensional stability	(Siró and Plackett, 2010; Mousa, Dong and Davies, 2016)
Barrier properties	Shelf life extension, Down-gauging films, Implants	(Lavoine *et al.*, 2012; Österberg *et al.*, 2013)
Medical	Drug delivery and controlled release, Scaffold in tissue engineering, Implants	(Dumanli, 2017; Xue, Mou and Xiao, 2017)
Aerogels	Self-healing materials	(De France, Hoare and Cranston, 2017)
Electronics	Time-temperature integrator, Freshness integrator, Gas and Leakage detector, Sensors and monitoring, Signal processor for biochemical pathways	(Kaushik and Moores, 2016)

In addition to lignin applications mentioned in **chapter 2.1**, nano-scaled lignin has also gaining attention. That said, the research in nanolignin applications is still in its early stage and commercialized products have not been reported yet, however potential applications are already proposed e.g., in the field of nanocomposites and

nanoparticles **(Table 3).** Many applications found in the literature is concentrated around improving mechanical properties of polymer composites, antioxidant and antibacterial properties, drug delivery, and energy storage via nanolignin carbonization.

Table 3. *Potential applications derived of nano-scaled lignin.*

Application	Reference
Structural reinforcement	(Nevárez *et al.*, 2011; Farooq *et al.*, 2019)
Ultraviolet blocker	(Yearla and Padmasree, 2016; Qian *et al.*, 2017; Farooq *et al.*, 2019)
Biocide	(Zimniewska, Kozłowski and Batog, 2008; Popa *et al.*, 2011; Gîlcă and Popa, 2013)
Antioxidant/Radical scavenging	(Lu *et al.*, 2012; Farooq *et al.*, 2019)
Pickering emusions	(Qian, Zhang, *et al.*, 2014; Nypelö, Carrillo and Rojas, 2015; Sipponen, Smyth, *et al.*, 2017)
Carbonized lignin particles	(Gonugunta *et al.*, 2012; Hu *et al.*, 2014; Lai *et al.*, 2014; Yiamsawas *et al.*, 2017)
Drug delivery (hollow particles/capsules)	(Tortora *et al.*, 2014; Yiamsawas *et al.*, 2014; Chen, Dempere and Tong, 2016)
Drug delivery (solid and porous particles)	(Dai *et al.*, 2017; Figueiredo *et al.*, 2017; Mika H. Sipponen *et al.*, 2018)
Enzyme immobilization	(Mika Henrikki Sipponen *et al.*, 2018; Capecchi *et al.*, 2019)

5. Nanocellulose and lignin interactions

While cellulose and lignin are investigated intensively, there are also studies elucidating the interaction between these lignocellulose constituents and potential value they can bring in combination likewise to their role as components of natural wood composites. Rojo et al. (2015) elucidated the effect of residual lignin on properties of nanocellulose-based films that exhibited faster dewatering during the film preparation process and higher WCA after hot press when lignin was present (Rojo *et al.*, 2015). Liu (2018) on the other hand utilized carboxylated nanocellulose

and industrial lignin exhibiting e.g., better colloidal stability of CNF dispersion and higher mechanical properties of nanocomposite films when lignin nanoparticles were present compared to residual lignin containing CNF films (Liu, 2018). Wang et al. (2018) investigated the effect of lignin on the properties of CNF and CNF-based nanofilms exhibiting higher tensile strength and wet strength in the presence of lignin. Moreover lignin had an increasing effect on contact angle results of CNF nanofilms (Wang *et al.*, 2018). Finally Farooq et al. (2018) utilized variety of different lignin morphologies with CNF revealing increased mechanical properties of nanocomposite films when spherical colloidal lignin particles were used. Moreover, spherically shaped CLPs made the nanocomposite films waterproof, and provided UV-shielding and antioxidant properties. They postulated that the reason behind the waterproofing phenomena is that CLPs block the pores between CNF constituents, reducing the permeability of water molecules (Farooq *et al.*, 2019). The tensile properties of studies discussed above are summarized in **Table 4**. The highest stress at break were reported by Wang et al. (2018) while the highest strain at break was achieved by Farooq et al. (2018). However, direct comparison of these results is not straightforward due to differences in analytical approaches.

Table 4. *Tensile properties of CNF nanocomposite films found from literature.*

Composite constituents	**Stress at break (MPa)**	**Strain at break (%)**	**Reference**
CNF +10% CLPs	160	16	(Farooq *et al.*, 2019)
Carboxylated CNF + lignin nanoparticles	245	15	(Liu, 2018)
Residual lignin-containing CNF (Eucalyptus)	250	4.9	(Herrera *et al.*, 2018)
Residual lignin-containing CNF (tobacco stalk)	255	11	(Wang *et al.*, 2018)
Residual lignin-containing CNF	116-164	1.7-3.5	(Rojo *et al.*, 2015)

6. Summary of the literature part

There has been a huge interest towards using biomass as a source of renewable energy and materials due to price increase of crude oil and obvious environmental concerns. The interesting chemical structure and high availability of cellulose and lignin makes them attractive as alternative options for petroleum-based products. The biomass-based nanomaterials are extensively studied and new techniques and morphological varieties are developed.

Depending on the preparation method, cellulose can be fractionated into nano-scale with different forms e.g. cellulose nanofibrils (CNFs), cellulose nanocrystals (CNCs), or bacterial cellulose (BC). The impressive properties of nanocellulose such as biodegradability, non-toxicity, low thermal expansion coefficience, high aspect ratio, and good optical properties has potential in many fields e.g. paper and packaging, medical and electronics.

Lignin has long been under shadow of cellulose due to its challenging chemical structure due to which lignin has been mostly used as a source of energy. Lately, many studies have showed ways to produce lignin nanoparticles in order to have a better control over the heterogeneous structure for further advanced applications such as dispersants, additives, binders and carbon fiber production. Moreover, nanoscaled lignin is also receiving increased attention as a strengthening agent in polymer composites, antioxidant and antibacterial applications, drug delivery and electronic applications through carbonization process.

As the knowledge on cellulose and lignin is increasing individually, many studies have also attempted to understand their interaction through composites. In fact, studies show that different lignin morphologies may bring additional value to the CNF films e.g. enhancing mechanical properties, wetting properties, and providing UV shields and antioxidant properties. This thesis attempted to increase understanding of the relationship between HefCel, a new type of nanocellulose, and spherical lignin particles to gain further knowledge on cellulose-lignin interactions.

EXPERIMENTAL PART

7. Aims of the work

The hypothesis of this master's thesis was that comparison of slow and fast nanofilm preparation methods will reveal new information regarding interactions of nanocellulose and nanolignin as well as resulting structure formation.

Moreover, this thesis also attempted to elaborate whether spherical colloidal lignin particles (CLPs) and the distinct morphology of HefCel (a type of nanocellulose) affected properties of the composites. In order to achieve this objective, the following sub goals were set:

- Characterization of the nanocomposite films with microscopy, tensile testing, and water contact angle measurements. The nanocomposite films were prepared using bleached HefCel and HefCel containing residual lignin.
- Assessment of the enzyme laccase as a tool to modify surface properties and tensile strength of the composite films

8. Materials and methods

Tensile properties of CLP-HefCel composites with different CLP content under wet and dry circumstance were examined. Wetting properties and effect of film formation method was also assessed. Additionally, residual lignin-containing HefCel (LigHefCel) was treated with enzyme laccase in order to evaluate its effect on tensile strength and surface properties of the composite films. The summary of the experiment procedure and materials used in this Master's thesis are presented in **Figure 23** and **Table 5**, respectively.

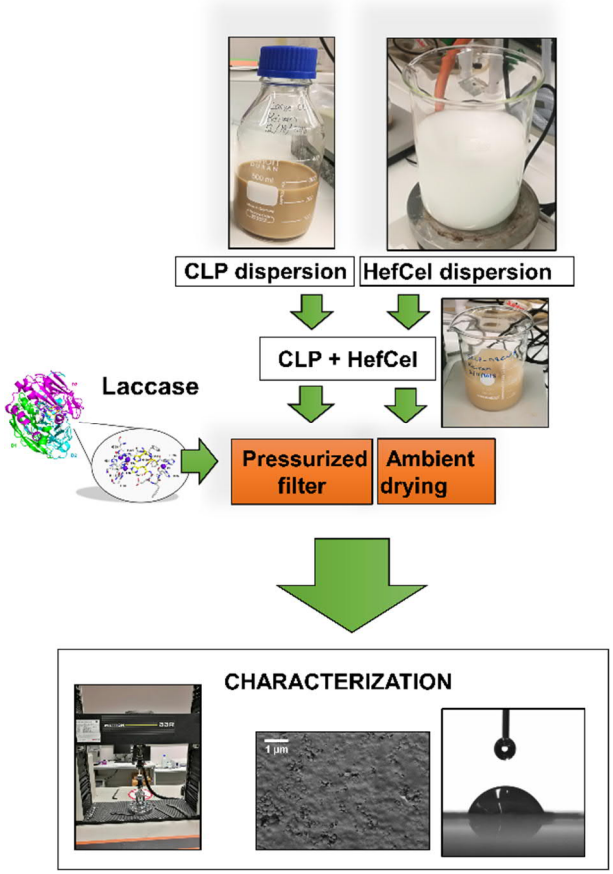

Figure 23. Schematic presentation of the experimental procedure. Model of laccase was adapted from Mate and Alcade (2015).

Table 5. List of materials used

Material
UPM BioPiva 200 Kraft lignin powder (batch # 8068-05-01, dry matter content 67.7 w%)
Tetrahydrofuran (100%, VWR Chemicals, density 0.888 g/ml)
HefCel (24.9.2018, bleached, HC 365, dry matter content 19.92 w%) *
HefCel (27.9.2018, unbleached, HC 370, dry matter content 16.98 w%) *
HefCel (24.9.2018, bleached, HC 386, dry matter content 22.34 w%) *
Laccase (3,5 mg/ml ja aktiivisuus 6500 nkat/ml, *Trametes hirsuta*) **
Sefar Nitex 10 µm 03-10/2
Whatman (Glass microfiber filters, GF/F, 0.7 µm)
Whatman (GF/A, 1,6 µm)
VWR 516-0834
Deionized water (DI-water)
Spectra/Por® 1 Standard RC Dry Dialysis Tubing, 6–8 kDa, Spectrum Labs, USA
Polyethylene low density petri dish

* The HefCel material was produced by VTT Technical Research Center of Finland.

** Laccase-enzyme was provided by VTT Technical Research Center of Finland.

8.1. Preparation of colloidal lignin particle dispersion

The preparation method of colloidal lignin particles was adapted from Lievonen et al. (2016) by carrying out CLP formation by fast nanoprecipitation instead of dialysis, as showed in **Figure 24** (Lievonen *et al.*, 2016; Sipponen, Smyth, *et al.*, 2017). The preparation process was initiated by dissolving (2.542 g) UPM BioPiva 200 Kraft lignin powder by mixing DI-water (17.2 g) and –tetrahydrofuran (THF, 58 ml). The black colored Kraft lignin solution was filtered through glass microfiber filter (Whatman GF/F, pore size 0.7 µm) to separate undissolved lignin. Filtered product was precipitated to form colloidal spheres by adding to DI-water (153.9 g) rapidly while stirring. Further, THF was removed by dialysis using dialysis membrane (Spectra/Por® 1 Standard RC Dry Dialysis Tubing, 6–8 kDa, Spectrum Labs, USA). The dialysis tubes filled with CLP suspension was placed in a bucket filled with DI-water and placed on a magnetic stirrer under a fume. The dialysis water was changed every 3 hours until the THF is removed from the CLP dispersion (at least 24 h), which is then followed by filtration through glass microfiber filter (Whatman GF/A, pore size 1.6 µm). For further characterization, the sizes of the particles where measured using dynamic light scattering (DLS) technique and the morphology was determined by taking transmission electron microscopy (TEM) images.

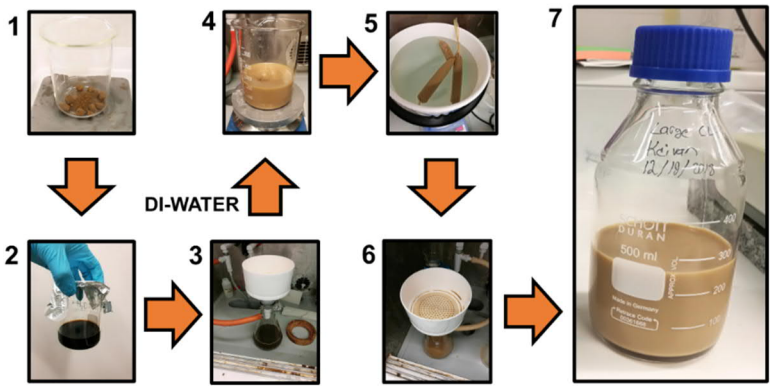

Figure 24. Preparation process of colloidal lignin particles from Kraft lignin to characterizing the finished CLP dispersion. 1) Weighting of kraft lignin 2) Lignin dissolution (DI-water + THF) 3) Filtration (GF/F) 4) Precipitation in water 5) Dialysis 6) Filtration (GF/A) 7) final CLP dispersion.

The dry content of CLP and HefCel dispersions was carried out by first weighting two empty vials and then vials containing the sample. The samples were placed in an oven for overnight (105 °C). The next day the vials containing dry samples were weighed, and the dry content was calculated using the following formula:

$$Dry\ matter\ content\ (\%) = \frac{m3 - m1}{m2 - m1} \times 100\ \%$$

Where $m1$ = empty vial, $m2$ = vial containing sample before drying in the oven, $m3$ = vial containing dry sample after overnight in oven. The final w % is the average of the two samples.

8.2. Preparation of HefCel dispersion

The paste like HefCel was diluted to 0.8 w% for further film preparation process using the following formula:

$$c1 \times m1 = c2 \times m2$$

where $c1$ is dry content of HefCel, $m1$ is the mass of the HefCel, $c2$ is the final concentration, and $m2$ is the total mass of water and HefCel. **Figure 25** shows the dilution process where ~ 4 g of HefCel (bleached) and 4,8 g of HefCel (unbleached) was mixed with approximately 96 g and 95 g of deionized water (DI-water) respectively, using a magnetic stirrer for approximately 2 h until it was homogenized. The suspension was preserved in a cold room at 4 °C.

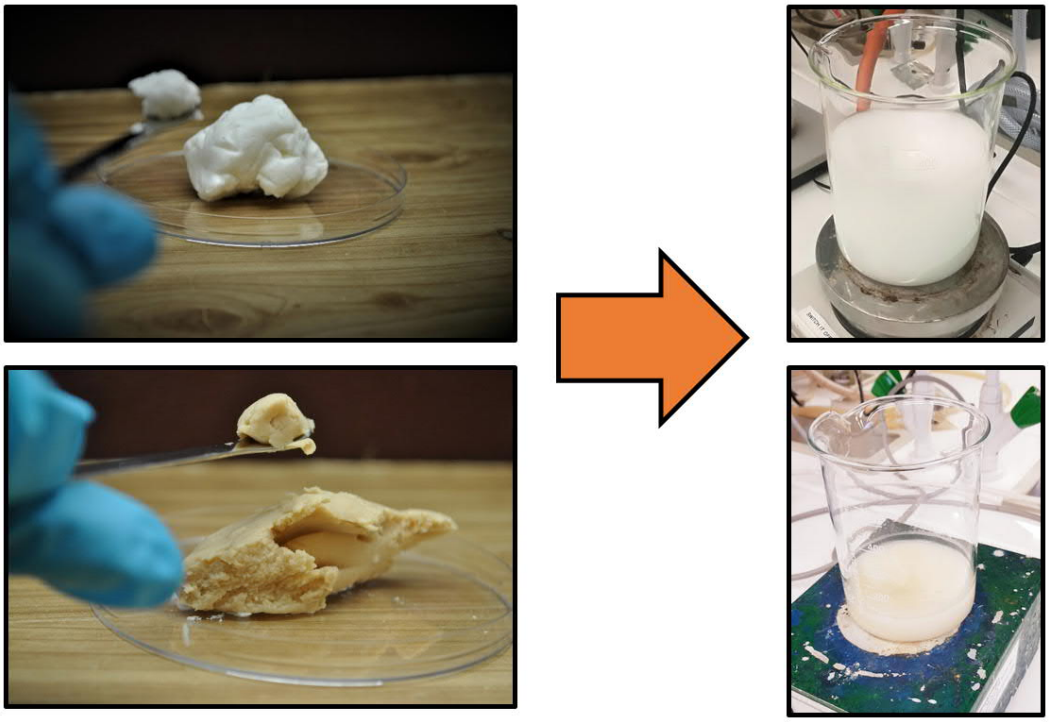

Figure 25. Preparation of HefCel (above) and residual lignin-containing HefCel (L-HefCel) (below) suspensions.

8.3. Preparation of CNF-composite films

The HefCel composite film preparation takes place after the CLP and HefCel dispersion is ready. The 100 ml of HefCel and 100 ml of CLP dispersions are mixed in order to get a suspension with CLP dry content of 0 w%, 1 w%, 5 w%, 10 w%, 15 w%, and 25 w%. The nanocellulose composite films were prepared by pressurized filtration adapted from a procedure recorded by Österberg et al. (2013) and solvent casting also refered as ambient drying method, which was performed by VTT to see whether the preparation method has an effect on the final properties of the films. (Österberg *et al.*, 2013) In **Table 6** the samples for both filtration method and ambient drying are summarized.

***Table 6**. The CLP-HefCel composite films prepared by pressurized filtering method and ambient drying method.*

Sample name	CLP (w%)	HefCel (w%)
HefCel	0	0.8
1CLP- HefCel	1	0.8
5CLP- HefCel	5	0.8
10CLP- HefCel	10	0.8
15CLP- HefCel	15	0.8
25CLP- HefCel	25	0.8

8.3.1. Nanocomposite film preparation via pressurized filtration and ambient drying method

The preparation of nanocellulose via pressurized filtration was initiated after the CLP-HefCel dispersion has been gently stirred on a magnetic stirrer for 15 minutes. The filtration equipment **(Figure 26, left)** is set up so that the dispersion is filtered through a Sefar Nitex sheet with pore size of 10 µm, which is placed on top of the VWR grade 415 filter paper. Furthermore the over pressure is slowly increased to 2.5 bar and maintained constant for 45 minutes. After the filtration process is ready, the wet films were ambient dried under a load of 5 kg for 72 h at 23 °C and 50% relative humidity. Ambient drying techique was applied by placing CLP-HefCel dispersion on a low-dencity polyethylene (LDPE) petri dish for 2-7 days at a room temperature for drying **(Figure 26, right)**.

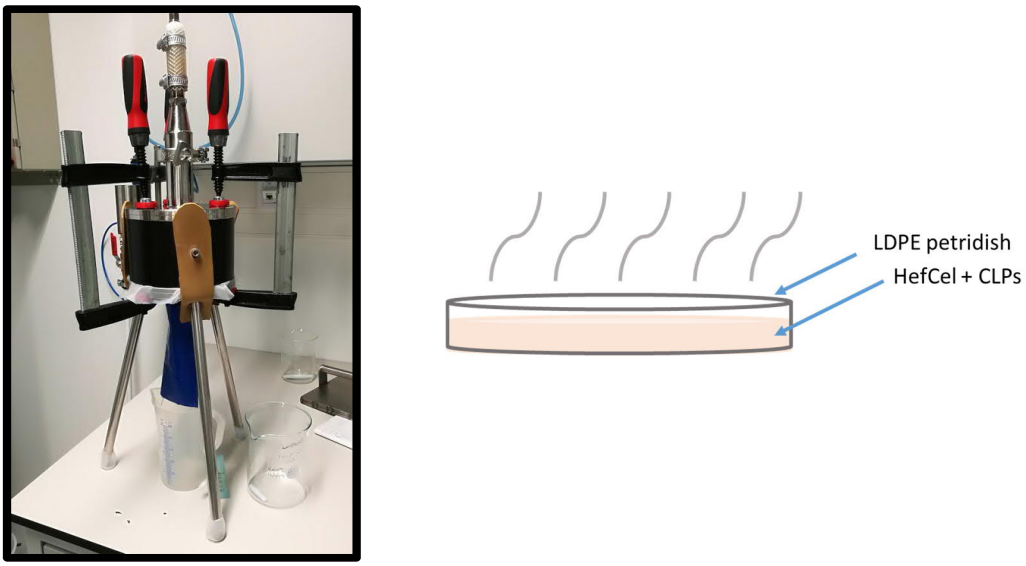

Figure 26. The filtration equipment (left) used in the preparation of nanocellulose films and schematic illustration of ambient drying setup (right).

8.3.2. Nanocomposite film preparation via pressurized filtration method with introduction of laccase-enzyme

Laccase enzyme was introduced to dispersion of CLP dry weight of 10 % and residual lignin containing HefCel (LigHefCel) to see whether crosslinking occurs between lignin constituents (residual lignin and CLPs) and whether it will have an effect on the properties of the composite films. The laccase with concentration of 3.5 mg/ml and activity of 6500 nkat/g was diluted to 50 nkat/g, 500 nkat/g, 1000 nkat/g, and 5000 nkat/g. The composite films with laccase was prepared using the filtration process described earlier in chapter 7. However, the procedure differed slightly as the laccase was added during the filtration process after 90 % of the suspension water had been filtered. The laccase was introduced this way in an attempt to spread the enzyme preparation evenly during the water flow. In total, seven films were prepared according to **Table 7** and **Figure 27**. From now on CLP with e.g. dry content of 10% is referred to 10CLP, whereas 500LAC means laccase with activity of 500 nkat/g.

***Table 7**. LigHefCel films from the laccase experimental series.*

Sample name	CLP (w%)	Laccase (nkat/g)
LigHefCel	0	0
LigHefCel-10CLP	10	0
LigHefCel-500LAC	0	500
LigHefCel-10CLP-50LAC	10	50
LigHefCel-10CLP-500LAC	10	500
LigHefCel-10CLP-1000LAC	10	1000
LigHefCel-10CLP-5000LAC	10	5000

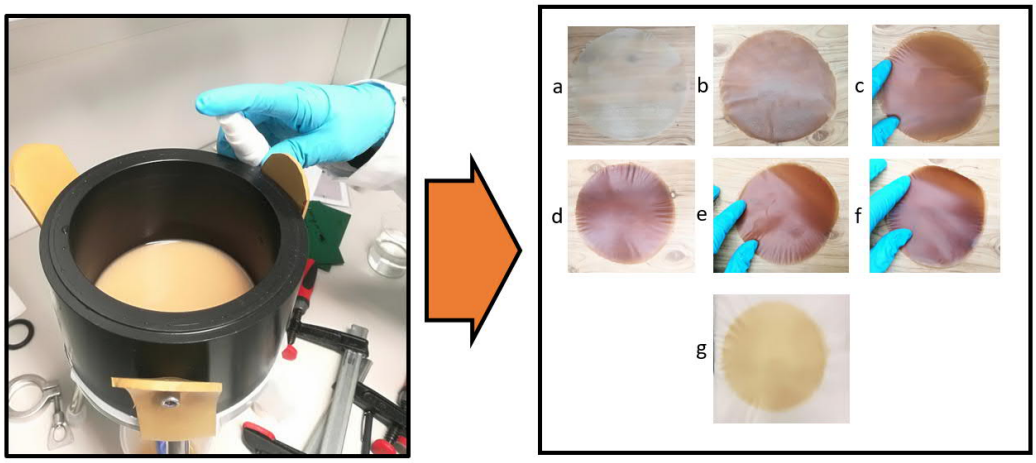

Figure 27. Films with laccase enzyme. Laccase enzymes are sprayed on the CLP-LigHC suspension (left). Series of films prepared: **a)** LigHefCel-500LAC **b)** LigHefCel-10CLP **c)** LigHefCel-10CLP-50LAC **d)** LigHefCel-10CLP-500LAC **e)** LigHefCel-10CLP-1000LAC **f)** LigHefCel-10CLP-5000LAC **g)** LigHefCel.

8.4. Characterization of nanocomposite films

Several different tests were applied to the films to understand the interactions between CLPs and HefCel and to evaluate the differences between preparation methods. These tests included measurements of tensile stress, water contact angle, and microscopy. Furthermore, the results are compared with other literature to distinct the differences between the new type of nanocellulose; HefCel and standard CNF.

8.4.1. Mechanical characterization

Mechanical properties of HefCel based composites were analyzed using Instron 4204 tensile tester, U.S.A. to measure the tensile stress and strain at break. The measurement was made using a 100 N load cell and 1 mm/min strain rate. Rectangular strips with known thickness were cut with dimensions of 50 x 5 mm^2 and equilibrated in 50% relative humidity and 23 °C for 48 h. Moreover, the edges at the longitudal ends of the strips were taped to avoid slippage in the tensile grips. (Farooq *et al.*, 2019) **Figure 28** is an example of the tensile equipment setup presenting strips before and after the tensile test.

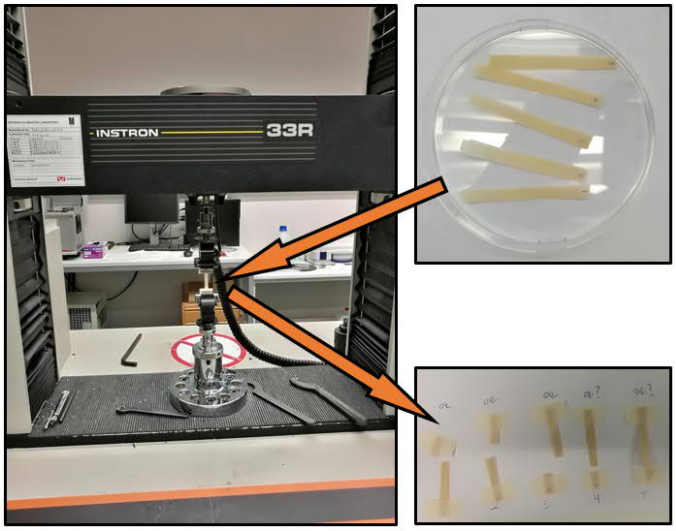

Figure 28. Setup of tensile machine where samples are pulled vertically to measure both stress and strain.

Moreover, the wet strength of composite films was tested. The samples were prepared by placing them into DI-water for 24 h. During the tensile strength measurements, the soaked samples were directly placed gently with tweezers between the clamps of the tensile-testing machine.

8.4.2. Measurements of water contact angle

Static water contact angle measurements were conducted to evaluate the wetting properties of the composite films.. During the wetting experiments KSV CAM 200 instrument was utilized (**Figure 29**). The instrument was set to drop water droplet with size and dropping rate of 6.5 µl and 1 µl/s respectively. Moreover, 30 frames were taken at 1s interval. The WCA were analyzed using Young/Laplace fitting method (Adamson and Gast, 1997). Moreover, Statistix9 software was used for statistical analysis (ANOVA).

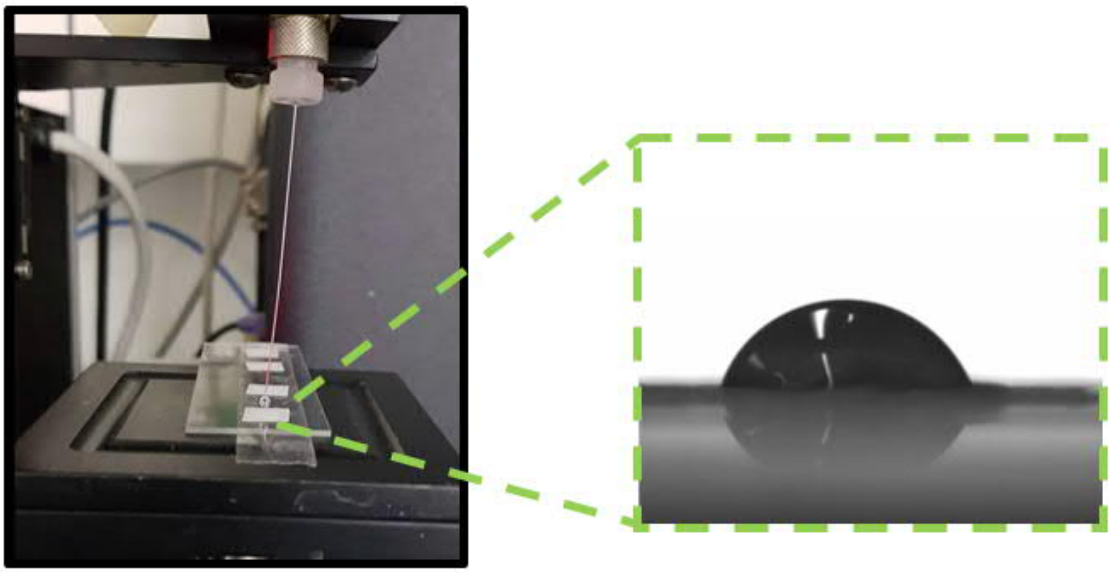

Figure 29. Contact angle measurement. Equipment setup, where water droplet is falling on the sample.

The measurements were applied to all samples at 3 different positions and both sides of each HefCel- and nanocomposite film. The dimension of the sample were 5 mm x 5 mm. The final contact angle value was determined by choosing the WCA-value at 10s and calculating the mean between both sides. Each sample was attached carefully from the edges on a glass plane with two-sided tape to avoid curling of the

sample, which is due to the hydrophilic nature of the composite. Further, gloves were used to avoid surface-contamination.

8.4.3. Microscopy and particle size measurement

Particle size of CLPs were determined using dynamic light scattering (DLS, Malvern Zetasizer). Before the particle size measurement could take place by using DLS, the samples were diluted to 1:20 using DI-water. Additionally transmission electron microscopy (TEM) and scanning electron microscopy (SEM, Sigma VP Zeiss) was used to characterize the morphology of the CLPs and surface morphology of HefCel and CLP-HefCel composite films, respectively.

Microscopy analysis of raw materials and thin films

The samples for SEM imaging was prepared by attaching on a carbon tape and further coating them with gold palladium (Au/Pd) using 30 mA current for 1:30 min (Sputtering equipment: Emitech, K700X). Micrographs of surface morphology of nanocomposite films were acquired with accelerating voltage of 5 or 1,5 kV and working distance of 5-7 mm. **Figure 30** shows the sample installation, sputtering instrument, and SEM instrument. In order to acquire TEM-image, CLP and HefCel dispersions were placed on a carbon based mesh grids and dried under ambient conditions. Furthermore, the images were taken by using bright-field mode on a FEI Tecnai 12 operating at 12 kV.

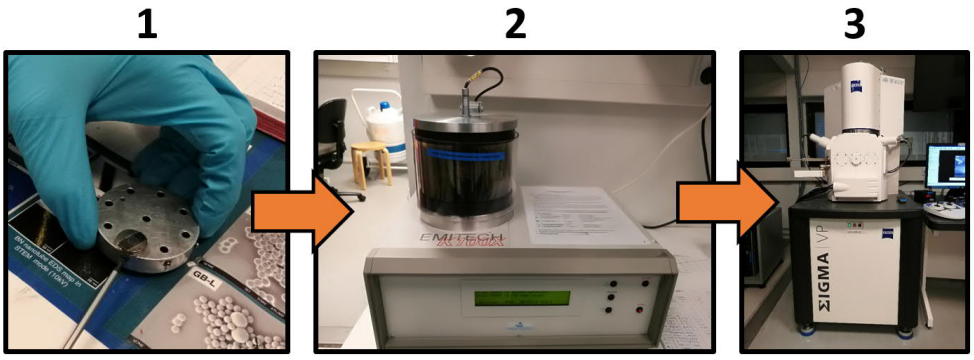

Figure 30. Surface morphology characterization of HefCel / CLP-HefCel films. 1) Preparation of the sample 2) Coating the sample with gold-palladium using sputtering instrument 3) Analyzing images using SEM instrument.

9. Results and discussion

Herein the results of nanocomposite film characterization including microscopy, tensile properties, and wetting properties of CLP-HefCel composite films are described in order to elucidate the properties of the thin nanocomposite films and further to have a better understanding of the CNF and CLP interactions.

9.1. Characterization of nanocellulose and nanolignin materials

Nanocomposite films prepared by filtration method exhibited both transparent and non-transparent films **(Figure 31)**. The less transparent films **(Filgure 31 c, e)** are considered to be defected due to the presence of incompletely fibrillated pulp fibres or aggregation of the fibrils, which might be the reason for the different arrangement of the fibrils and further having dissimilar effect on light transmittance.

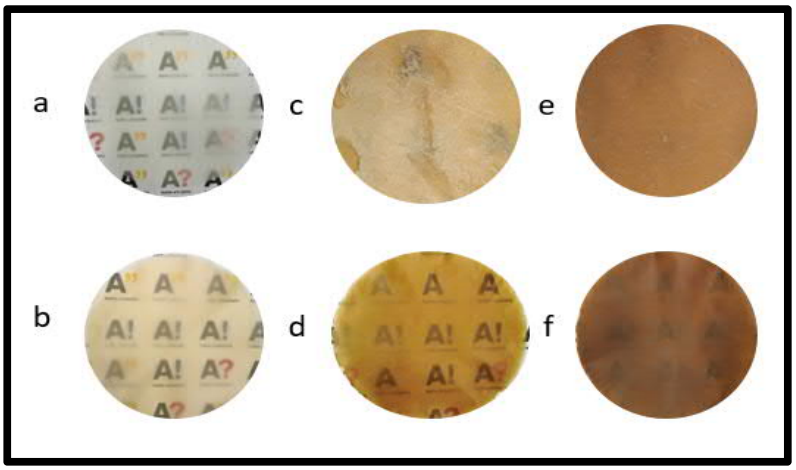

Figure 31. Nanocellulose composite films prepared by pressurized filtration: a) HefCel, b) 1%CLP-HefCel c) 5%CLP-HefCel d) 10%CLP-HefCel e) 15%CLP-HefCel f) 25%CLP-HefCel.

The nanocomposite films prepared by ambient drying method, exhibited relatively good transparency thus less defected fibrils **(Figure 32)**. Moreover, the color intensity increase with the increasing amount of lignin.

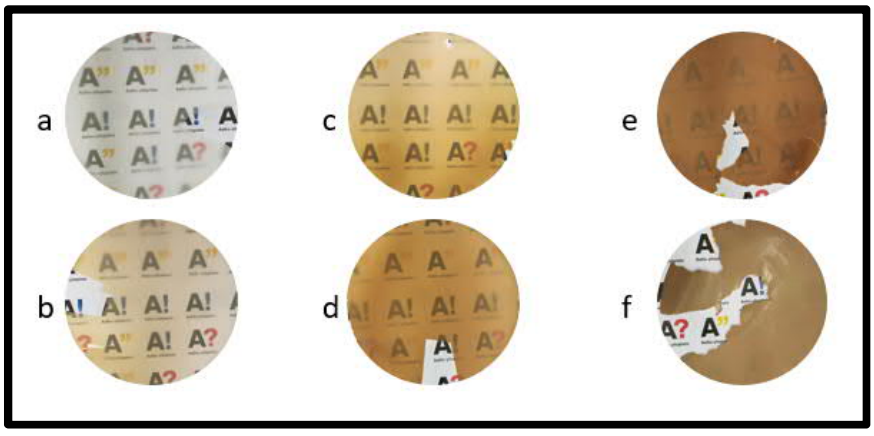

Figure 32. Nanocellulose composite films prepared by suspension casting. a) HefCel b) 1%CLP- HefCel c) 5%CLP-HefCel d) 10%CLP- HefCel e) 15%CLP- HefCel f) 25%CLP-HefCel. Missing pieces in a-d are due to sample measurement, whereas e and f nanocomposite films are missing pieces due to adhesion with LDPE petri dish.

Schematic illustration was created of CLPs and HefCel-fibrils based on a hypothesis that CLPs are spread homogenously in the HefCel matrix **(Figure 33).**

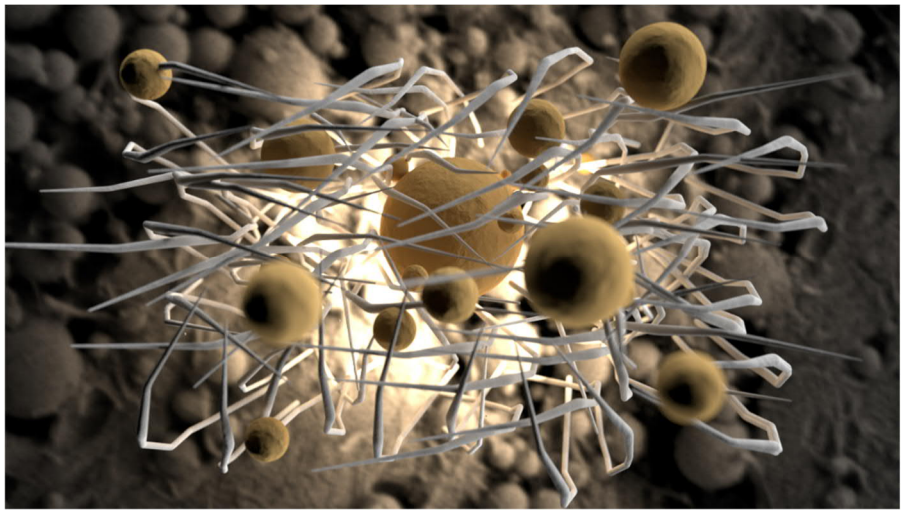

Figure 33. *A schematic model of CLP-HefCel interaction. Brown spheres represent CLPs and white fibrils represent HefCel. The background image was taken with SEM representing 10CLP-HefCel composite. This image was made with Blender software.*

Characterization of the nanoscaled materials by transmission electron microscopy (TEM) was made to determine the morphology of diluted bleached HefCel, unbleached HefCel, and CLPs. TEM images of HefCel and LigHefCel exhibited individual fibrils with diameter and length of 20 nm and 500 nm respectively and larger bundles with diameter of ca. 250 nm to 600 nm (**Figure 34**). Thus it can be concluded that the length of the individual HefCel fibrils was smaller than standard CNF mentioned in Chapter 3 whereas bundles of HefCel fibrils exhibited larger width. In addition to the individual and bundles of HefCel fibrils, larger and incompletely fibrillated cellulose fibers were observed. It can be concluded that the short nanofibrils of HefCel share some resemblance to CNCs, but the heterogeneous dispersion contains also microscaled cellulosic fibre parts. Although HefCel is produced mechanically, the cellulase enzyme assist the dissolution by cutting from amorphous regions of cellulose, which is similar to the acid treatment during the CNC

production. The final product with acid and cellulose treatment is a longitudinally shortened product.

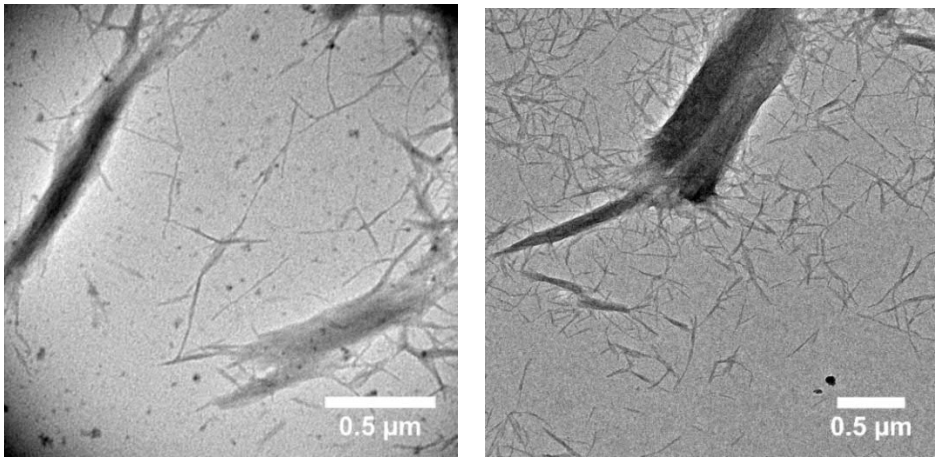

Figure 34*. TEM images of bleached HefCel (left) and HefCel containing residual lignin (right).*

TEM images of CLPS (**Figure 35**) displayed spherical lignin particles that appeared similar to those reported earlier by Lievonen et al. (2016). The diameter of the particles appeared to span from 50 nm to 300 nm. The DLS measurement displayed z-average diameter 200 +/- 3 nm and a PDI value of 0.227 with standard deviations of 2.94 and 0.016, respectively.

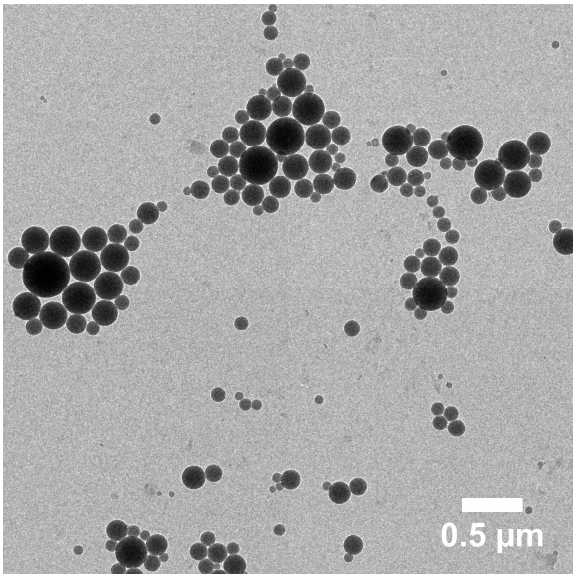

Figure 35. TEM image of CLP particles.

Investigation of the nanocomposite films

Scanning electron microscopy (SEM) was employed to determine the morphology and microstructure of bleached HefCel and LigHefCel nanocomposite films prepared by the filtration method. Furthermore, dispersibility of CLPs in HefCel matrix was also investigated in order to determine their relationship with HefCel-fibrils. In the absence of CLPs, both bleached HefCel and LigHefCel showed relatively smooth surfaces on which HefCel fibrils have aggregated on each other (**Figure 36)**.

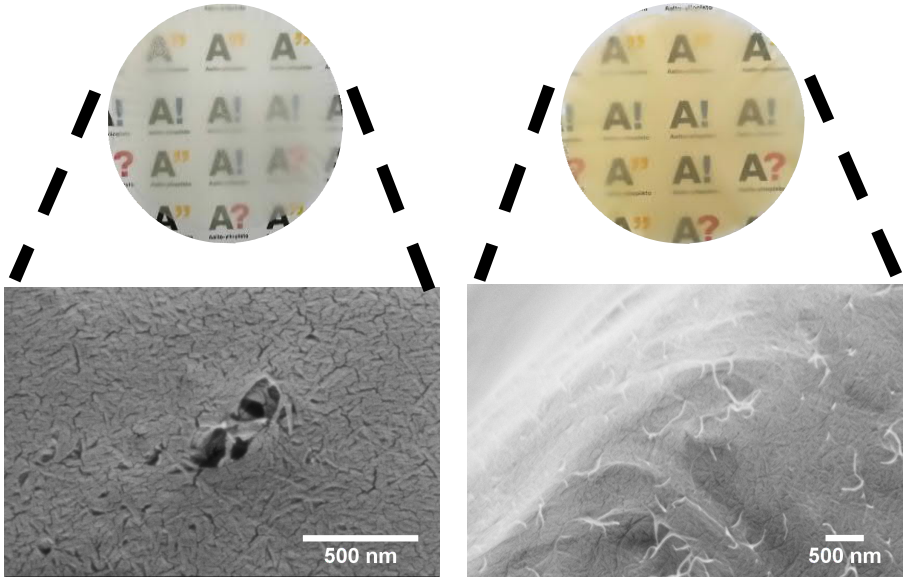

***Figure 36**. SEM images of bleached HefCel (left) and LigHefCel (right)*

Furthermore, SEM micrograph (**Figure 37)** shows that when 10 wt% of CLPs were mixed in the bleached HefCel dispersion, the CLPs were well dispersed in the resulting nanocellulose film matrix. Moreover, the particles did not show clear aggregating behavior and were mostly covered under a thin layer of HefCel fibrils.

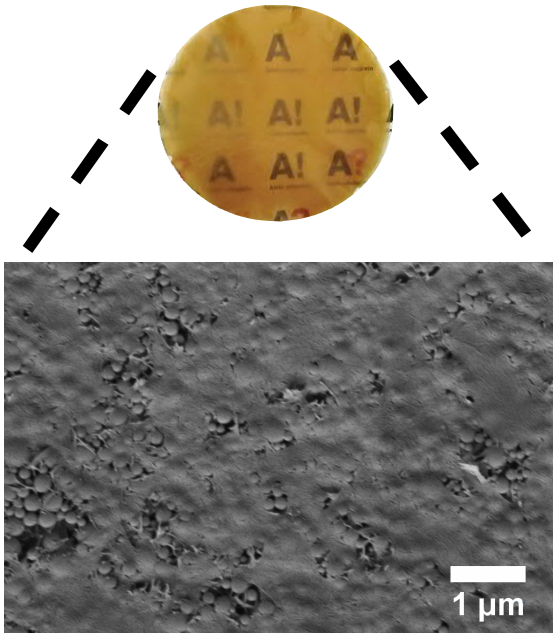

***Figure 37**. SEM image of HefCel nanocomposite film containing 10 w% CLP (10CLP-HefCel).*

The structural differences between defect and defect free nanocomposite films are presented in **Figure 38**. The left image of **Figure 38** is an example prepared by pressurized filtration method displaying irregularities on the surface of the nanocomposite film due to aggregated HefCel fibrils. Furthermore, nanocomposite film without irregularities are presented in right image in **Figure 38**, exhibiting finer fibrils which are adjusted according to the pattern of the Nitex sheet. The microscaled pattern on the nanocomposite film **(Figure 38, right)** is due to morphology of Nitex sheet. Furthermore, defected composite film (**Figure 38, left**) did not show as clearly the pattern of Nitex sheet due to coverage of aggregated HefCel fibrils.

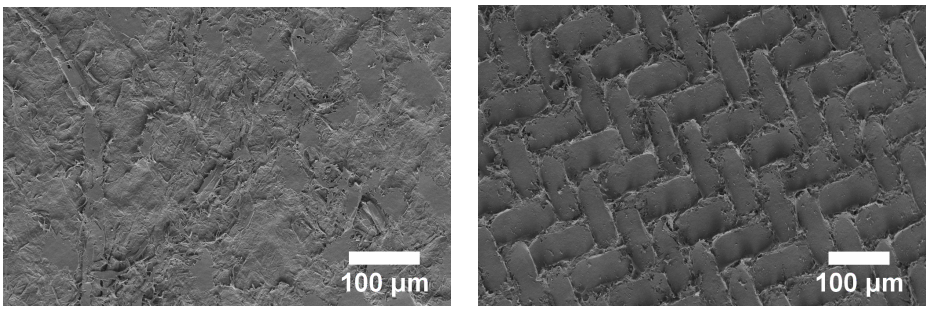

Figure 38. Morphological difference between defected nanocomposite film, which is due to aggregated HefCel fibrils during preparation(left) and defect free nanocomposite film (right). Both films contain CLPs.

9.2. Mechanical properties of nanocomposite films

In this chapter the tensile properties of HefCel/LigHefCel based nanocomposite films are discussed. First, the effect of preparation method of HefCel based nanocomposite films on their tensile properties is presented. Secondly, the wet strength results and finally the effect of laccase on LigHefCel-based nanocomposite films are discussed.

9.2.1. The influence of preparation method on HefCel-based nanocomposite film tensile properties

The stress strain curves of HefCel nanocomposite films prepared by pressurized filtration method and ambient drying method are compared in **Figure 39**. Pure HefCel nanocomposite film prepared by pressurized filtration **(Figure 39a)** demonstrated the largest stress at break value of 46 MPa, whereas addition of CLPs to the HefCel matrix resulted in tensile strength values between 19 MPa and 36 MPa, in inverse relation to the CLP content of the film. Moreover, CLPs did not have major influence on the strain at break value exhibiting only slight reduction compared to pure HefCel. It can be concluded from the stress-strain data above that the inclusion of CLPs had a negative, but non-linear effect on the tensile properties. In the case of ambient dried nanocomposite films **(Figure 39b),** addition of CLPs in range of 5-15 w% displayed enhancement to the tensile stress at break with values of 47-56 MPa, whereas 1% and 25% showed negative effect compared to the results of pure HefCel. Moreover, according to data above, it can be determined that the strain at break does not vary much between CLP-HefCel composites, however the data shows 25% reduction of elongation at break value when compared to pure HefCel. The stress at break data of both preparation methods are summarized in **Figure 39c** for further analysis.

To be able to analyze the stress at break graph sufficiently **(Figure 39c)** it is worth noting that appearance of surface-inhomogeneity on the 5%CLP-HefCel and 15%CLP-HefCel nanocomposite films prepared by pressurized filtration method (**APPENDIX 1**) presented a challenge to identify the trend in the mechanical properties. However, excluding these two defected samples from comparison a general reduction of tensile properties in the presence of CLPs was observed, originating from the disrupted hydroxyl bonding between the HefCel fibril. However, Farooq et al. (2018) showed recently that addition of CLPs at an optimum concentration of 10% increased the stress and strain of the nanocomposite films. It was hypothesized that CLPs act as ball bearing lubricants that can transfer stress and further enhance ductility and toughness of the films (Farooq *et al.*, 2019). That said the similar effect was not seen

in HefCel nanocomposites prepared by pressurized filtration method. It is hypothesized that it is due to the shorter fibrils in contrast with the longer and more conventional CNF used in Farooq et al. (2018).

Nanocomposite films prepared by ambient drying technique alternatively displays more obvious behavior, where CLP with 5 wt% reached the highest tensile strength, with slight increase as compared to the reference, after which the stress at break decreased quite linearly with increasing CLP content. This heavy declining behavior is similar to Farooq et al. (2018) study, where the authors found that optimum CLP content in CNF-based nanocomposite films (prepared with filtration method) for both unmodified CLPs and cationized CLPs (c-CLPs) is 10 wt%. Further increasing c-CLP concentration up to 50 wt%, resulted in a decrease in the strength of the nanocomposite films. They postulated that the reason for loss of mechanical strength was due to severe disruption of interfibrillar bonding due to excessive amount of CLPs. The hypothesis why HefCel-based nanocellulose films prepared by pressurize filtration and ambient drying technique did not behave similarly might be due the loss of CLPs during the filtration process. This hypothesis is supported by the brown color observed in the permeate during the filtration which indicated occurrence of lignin. This exclusion of CLPs in the filtration method and full retention in the evaporation approach may explain the difference in the mechanical properties of the films prepared by these two methods. Moreover, other reason for different mechanical properties between the preparation methods could be the different organization of the HefCel-fibrils. It is postulated that the external forces of pressurized filtration (over pressure) will affect the aligning of the fibrils differently than ambient conditions under which the constituents have greatly more time to orient according as the water evaporation took several days in contrast to dewatering in less than an hour during the filtration approach. The different alignment phenomena is also supported by the water contact angle measurements discussed in **Chapter 8.2.**

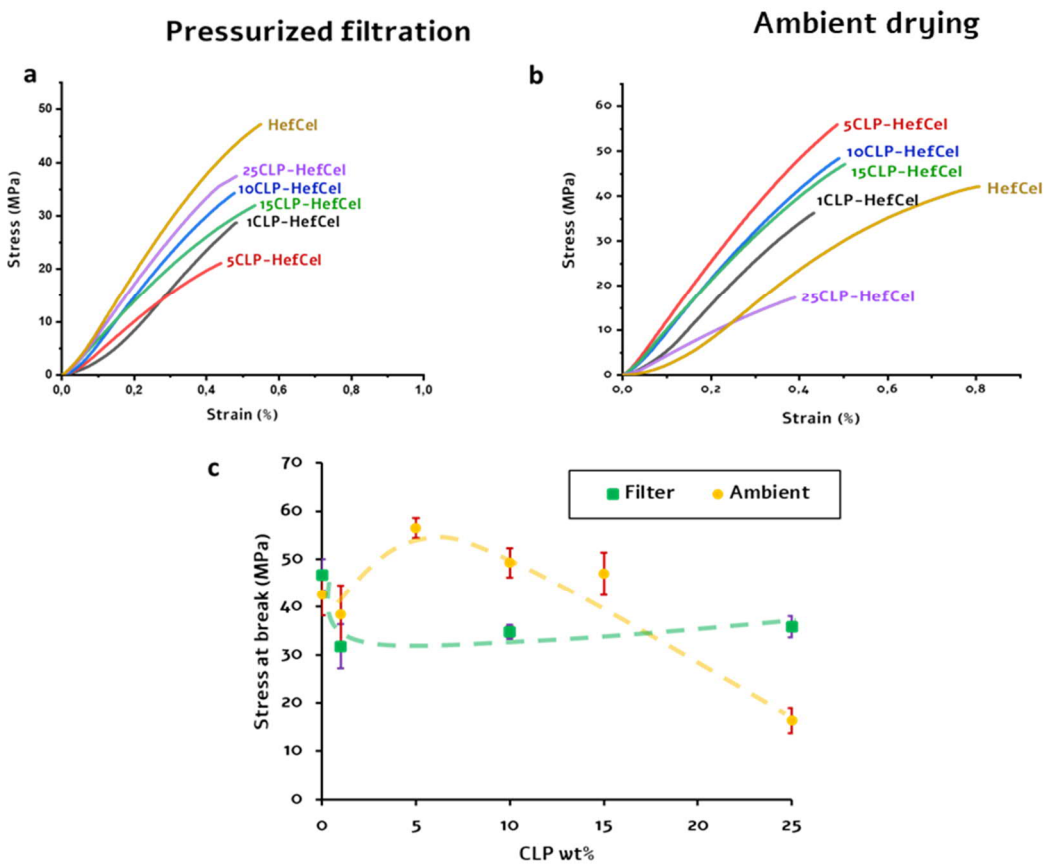

Figure 39. Representative tensile stress-strain curves of HefCel films containing 0-25% CLPs. (**a**) Films prepared by pressurized filter. (**b**) Films prepared by ambient drying. (**c**) Comparison between tensile stress at break of pressurized filtration method and ambient drying method. The defected nanocomposite films 5%CLP-HefCel and 15%CLP-HefCel prepared by pressurized filtration method were excluded due to their inhomogeneity in order to identify the trend more clearly. The dashed lines are shown only to indicate trends.

Generally, the tensile properties of CLP-HefCel based composites exhibited lower tensile properties than many earlier studies that have utilized regular CNF from non-enzymatically treated cellulosic fibers **(Table 4)**. Thus, it can be concluded that the lubricant effect of CLPs as proposed by Farooq et al. (2018) is more suitable to improving tensile properties of long CNF than the shorter HefCel, because

entanglement and longitudal interfibrillar hydrogen bonding are more abundant with the former mentioned.

Additionally, the wet strength test was conducted to a few samples to determine the effect of water to nanocomposite tensile properties. However, when samples were taken out from DI-water after 24 hours, they showed negligible strength below 0.1 MPa. In fact, the nanocomposite strips could not resist gentle handling required during inserting the specimens into the testing equipment. The hypothesis for weak wet strength of HefCel-based nanocomposite films is due to the above discussed insufficient fibrillary entanglements and overpowering effect of water molecules disrupting already weak forces between HefCel fibrils, which will cause short HefCel-fibrils to depart from each other, thus weakening the mechanical properties. Some studies however show that the wet strength properties of nanocellulose composites can be enhanced. For example, in a study of Lucenius, Parikka and Österberg et al. (2014) it was discovered that uncharged polysaccharides such as galactoglucomannan enhanced the wet strength of CNF based composites increasing the Young's modulus by a factor of 1.3 and tensile strength by a factor of 2.8 (Lucenius, Parikka and Österberg, 2014). Moreover, Quellmalz and Mihranyan (2015) were able to increase the wet strength properties of nanocellulose films by crosslinking the nanocellulose constituents with citric-acid (Quellmalz and Mihranyan, 2015). It is noteworthy, however that Quellmals and Mihranyan (2015) used a wet strength testing setup that was conducted in a much shorter water soaking time (15 min) whereas Lucenius et al. soaked the samples for 24 h, moreover both these studies used longer fibrils than in this study.

9.2.2. The effect of laccase enzyme on LigHefCel-based nanocompositefilms

Laccase was introduced to residual lignin containing HefCel (LigHefCel) and CLP composites in an attempt to form crosslinks between lignin constituents and to further evaluate whether it has an impact on the mechanical properties. The stress-strain curves of the films obtained from laccase-treated LigHefCel and its mixtures with CLPs is shown in **Figure 40**.

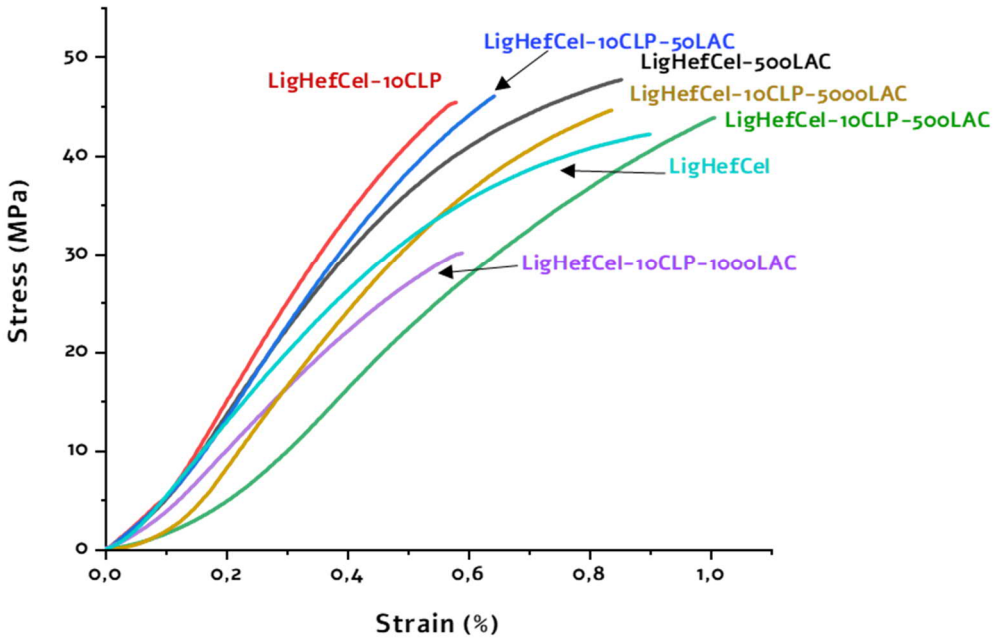

Figure 40. Stress-strain curve of nanocomposite films cointaining HefCel with residual lignin (LigHC), 10%CLP and LigHC

According to the data above the stress at break values were ranging between 40-47 MPa, where LigHefCel with CLP 10 wt% and laccase activity of 50 nkat/g (LigHefCel-10CLP-50LAC) presents highest stress at break value (47 MPa). Thus, it can be determined that laccase does not have much effect on the stress at break property when compared with the result in **Figure 39a**.

Moreover, the Young's modulus of the samples were calculated in order to determine whether crosslinking is taking place between lignin constituents **(Figure 41)**. Young's modulus is a measure of stiffness and it correlates with cross-linking density (Schlesing, Buhk and Osterhold, 2004). That said, according to variance analysis (one-way ANOVA) there are no significant pairwise differences among the means of the samples **(APPENDIX 2)**. Therefore, it is hard to say whether crosslinking was taking place. It can be also speculated that, whether the crosslinking is taking place or not, it is more likely that the crosslinking-effect would occur on the surface of the nanocomposite films. Therefore, the effect of crosslinking would not affect the strength of the whole nanocomposite film. Moreover, the effect of enzymatic crosslinking may not be able to compensate the weak tensile strength of the HefCel fibrils due to their short length. Laccase-catalyzed crosslinking has been observed as an increase in lignin molecular weight using gel permeation chromatography (GPC) measurements (Hortling, Turunen and Kokkonen, 1999). However, this analysis is out of scope of this Master's thesis.

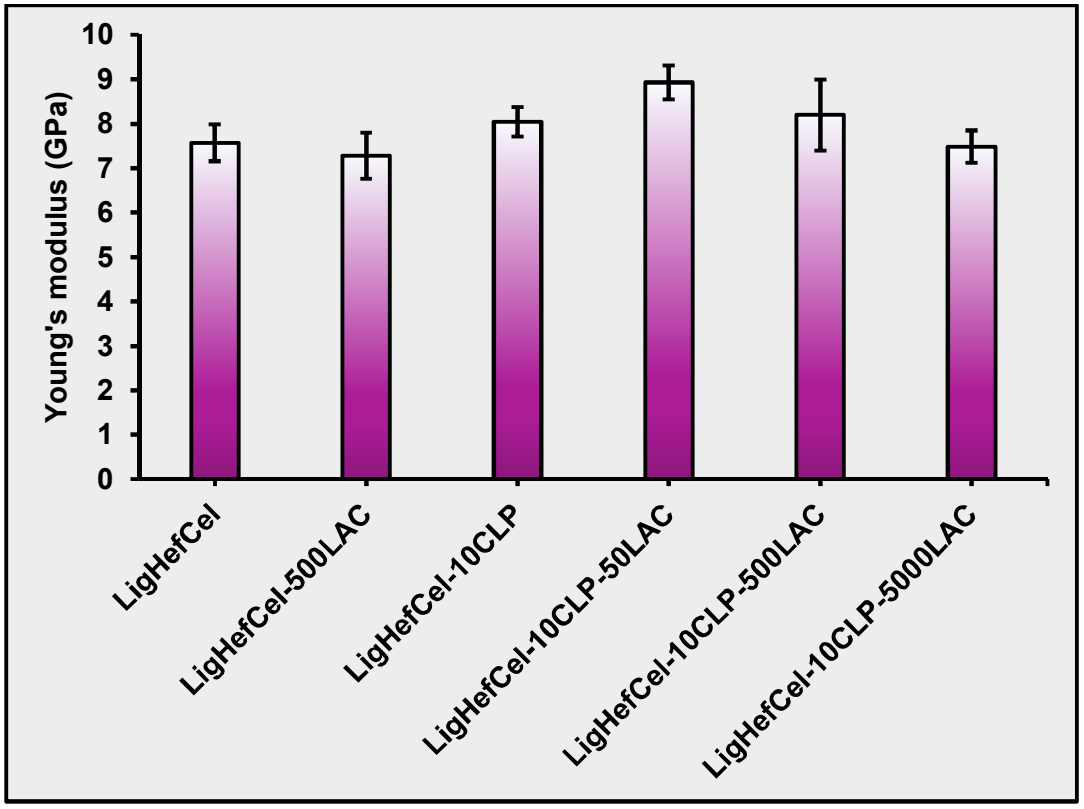

Figure 41. Young's modulus data of laccase experiments. LigHefCel-10CLP-1000LAC was excluded due to impurities on the surface of the film.

The tensile properties of residual lignin-containing HefCel (LigHefCel) were comparable to those of pure HefCel prepared by ambient drying technique indicated in Figure **39 b,c** and **Figure 40**, respectively. In fact, LigHefCel displayed higher strain at break when compared to pure HefCel prepared with the filtration-method. From industrial point of view, it would be beneficial to prepare LigHefCel for it is less chemical consuming than further bleaching the HefCel. That said, it depends on the application, for LigHefCel has distinct brownish color due to the residual lignin which might not be suitable for some applications.

9.3. Surface characterization of nanocomposite films by water contact angle testing

In this chapter the wetting behaviour of HefCel/LigHefCel based nanocomposite films are discussed. The discussion begins with comparing the effect of preparation method of HefCel based nanocomposite films on their wetting properties after which the effect of laccase on LigHefCel-based nanocompositefilms and their wetting properties are discussed. Detailed data is presented in **APPENDIX 4.**

9.3.1. The influence of preparation method on wetting properties of HefCel-based nanocomposite films

The wetting behavior of HefCel / LigHefCel nanocomposite films were determined by water contact angle (WCA) measurements. The contact angle measurements of nanocomposite films prepared by pressurized filtration method and ambient drying method are shown in **Figure 42**. Films from both preparation methods of nanocomposites displayed WCA below 90^{o}, thus exhibiting hydrophilic behavior. WCA of composite films prepared by the filtration method and ambient drying method ranged between 28^{o}-35^{o} and 40^{o}-50^{o}, respectively. The hydrophilic behaviour was expected due to the polar groups within the molecular structure of both HefCel and CLPs. However, different behavior can be identified between the preparation methods after setting a linear fit to the datasets. In case of filtrated composite films, it can be determined that the linear slope is almost zero indicating that CLP did not have a significant effect on the WCA. In addition, the coefficient of determination (R^2) was also low (0.01), which means that the predictability of linear fit was not reliable.

Nanocomposite films prepared with ambient drying method on the other hand displayed a clear declining slope with R^2 of 0,58. This was more reliable prediction on the relationship of CLPs and WCA, and passed the Student's t-test at a probability level of $p < 0.01$.

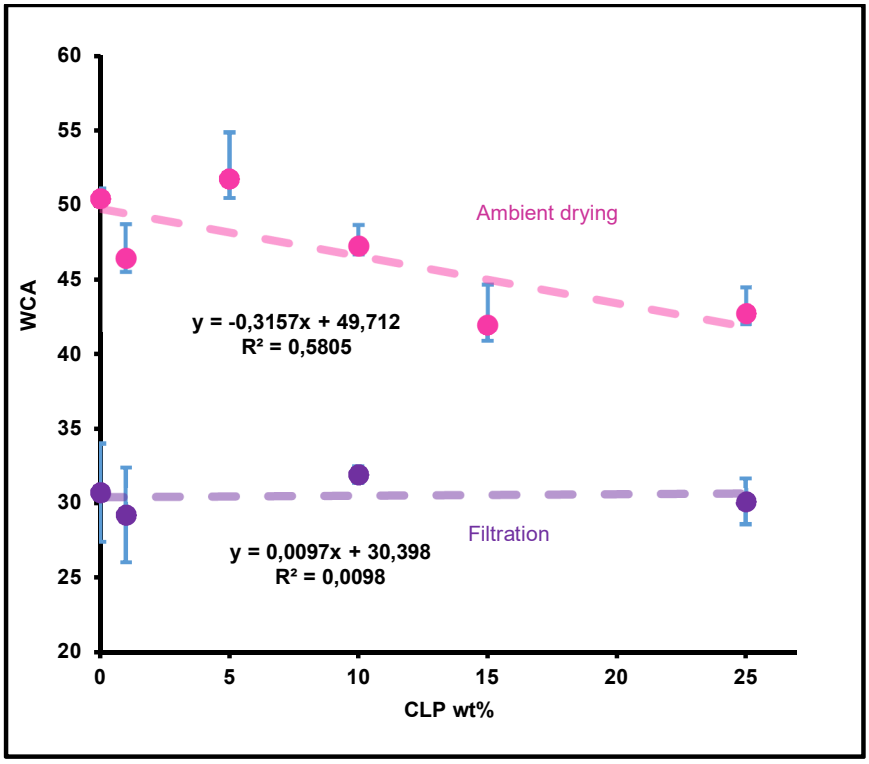

Figure 42. Water contact angle results between pressurized method and ambient drying method. Composites with CLP 5wt% and 15wt% prepared by filtration method was excluded from the graph due to appearance of irregularities.

It is hypothesized that the higher WCA found with nanocomposite films prepared by the ambient drying method compared to pressurized filtration method is due to different surface morphology. According to Cassie and Baxter (1944), WCA increases along with the surface roughness or appearance of air pockets (Cassie and Baxter, 1944). Thus it can be speculated that nanocomposite films prepared by ambient drying method promoted formation of air-pockets between protruding HefCel constituents on the surface due to water evaporation during the slow drying process. Moreover, the pattern of Nitex sheet formed on nanocomposite films during the filtration, which lacks in composite films prepared with ambient drying method, may also effect the WCA results. Furthermore, it is postulated that the reason behind the unreliable predictability of WCA trend of nanocomposite films prepared by pressurized filtration method is due to the loss of CLPs during the filtration process.

9.3.2. The effect of laccase enzyme on LigHefCel-based nanocomposite films

Water contact angle measurements were also conducted on LigHefCel-based nanocomposites with and without laccase treatment to investigate whether the enzymatic treatment had any effect on the wetting properties. The WCA results are presented in **Figure 43**.

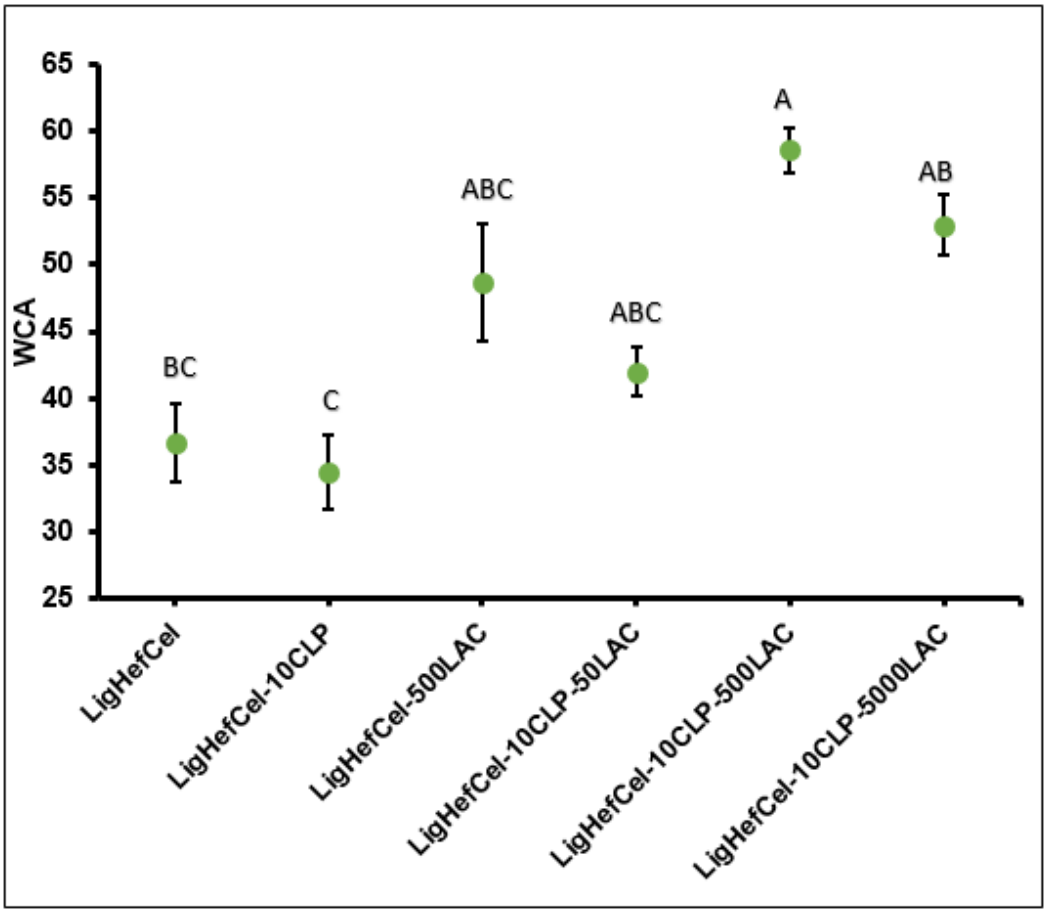

Figure 43. Water contact angle and ANOVA results of nanocomposites prepared by pressurized filtration method and addition of laccase enzyme. LigHefCel-10CLP-1000LAC was excluded due to irregular morphology on the surface of the film. Based on ANOVA and Tukey's HSD test, letters A, B, and C indicate groups that are not significantly different from the results marked with the same letter ($p < 0.01$).

Generally, films used in the laccase experiment displayed WCA between 35°–59° exhibiting higher values than found with HefCel-based nanocomposite films prepared

by the similar filtration method **(Figure 43)**. Moreover, the data above was analyzed using one-way ANOVA with Tukey's HSD test. **(APPENDIX 3)**. It can be concluded that LigHefCel-10CLP-500LAC significantly differs with LigHefCel-10CLP and LigHefCel. Furthermore, it can be determined that laccase has an increasing effect on WCA.

The high WCA values acquired from laccase experiments could be explained by the formation of quinone methides from lignin (explained in Chapter 2.3). The chemical structure of quinone methide is less hydrophilic than conventional lignin phenols, which might be the reason for the higher WCA than composite films without presence of laccase. Also the reddish color of laccase-containing nanocomposite films could be an indication of the occurrence of quinones, since for example guaiacol forms orange-red products after laccase-catalyzed oxidation **(APPENDIX 5)** (Jiang *et al.*, 2010).

10. Summary and suggestions for future research

During this master's thesis HefCel and colloidal lignin particle nanocomposite films were prepared with different methods (filtration and ambient drying) in order to get a better fundamental understanding of the interactions between CNF and lignin particles. Generally, tensile properties of HefCel-based nanocomposite films were low compared to literature values of more conventional CNF-based composites. Additionally, different trends were displayed between the pressurized filter and ambient drying methods. The latter produced films that exhibited higher tensile properties and exhibiting effect of lignin content on the tensile strength properties that was comparable to that of conventional CNF-based composite films used e.g. in a study by Farooq et al. (2018). It is hypothesized that the relatively weak tensile strength obtained with HefCel is due to the morphology and small size of the fibrils which prohibits the entanglement with each other. Moreover, the nanocomposite films were very weak in wet state, displaying sensitivity towards physical handling. Laccase experiment did not enhance the tensile properties nor did it display strong indication of cross-linking between the lignin constituents according to the Young's modulus results. However, a clear color formation in the films was observed, indicating that some oxidation reactions did take place.

Water contact angle values showed that the nanocomposite films had hydrophilic surfaces, but higher contact angles were recorded compared to the values of conventional CNF nanocomposite films used in the research of Farooq et al. (2018). It is hypothesized that this is due to the different morphology and arrangement of fibrils in the films. It can also be speculated that short HefCel-fibrils are able to orient in the z-direction and create air pockets thus enhancing the WCA values. Furthermore, laccase treatment of the films increased the WCA making the LigHefCel-based nanocomposites more hydrophobic compared to HefCel-based nanocomposites without laccase treatment. It is postulated that the reason for the

WCA enhancement is due to appearance of more hydrophobic quinone structures compared to initial phenolic lignin constituents.

In order to fully utilize the HefCel material, more research is required to discover its full potential at an application level. HefCel-based nanocomposite films may not possess enough tensile strength to challenge the conventional CNF-nanocomposite films by itself. However, HefCel fibrils might bring additional value when combined together with regular CNF, for it is postulated that small size of HefCel could potentially fill the gaps created by CLPs and CNF and further enhance the fibril-fibril bonds. Additionally, HefCel could increase the WCA values of CNF-based nanocomposite films. For further research, the oxygen barrier properties of HefCel based nanocomposite films could be analyzed in order to identify whether the films have potential for packaging applications. Furthermore, the effect of laccase could be evaluated more in detail using different spectroscopy measurements such as infrared spectroscopy and UV-Raman spectroscopy.

11. References

Abdul Khalil, H.P.S. Davoudpour, Y. *et al.* (2016) 'A review on nanocellulosic fibres as new material for sustainable packaging: Process and applications', 64, pp. 823–836. doi: https://doi.org/10.1016/j.rser.2016.06.072.

Adamson, A. W. and Gast, A. P. (1997) *Physical Chemistry of Surfaces*. 6th edn. New York.

Adler, E. (1977) 'Lignin chemistry - past, present and future.', *Wood Sci. Technol.*, 11(3), pp. 169–218. doi: https://doi.org/10.1007/BF00365615.

Ago, M. *et al.* (2016) 'High-Throughput Synthesis of Lignin Particles (30 nm to 2 µm) via Aerosol Flow Reactor: Size Fractionation and Utilization in Pickering Emulsions', *Applied materials and science*, 8(35), pp. 23302–23310. doi: 10.1021/acsami.6b07900.

Azeredo, H. M. C. *et al.* (2017) 'Nanocellulose in bio-based food packaging applications Ind Crops Prod, 97, pp. 664-671', *Industrial Crops & Products*, 97, pp. 664–671. doi: 10.1016/j.indcrop.2016.03.013.

Baurhoo, B., Ruiz-feria, C. A. and Zhao, X. (2008) 'Purified lignin : Nutritional and health impacts on farm animals — A review', *Animal Feed Science and Technology*, 144, pp. 175–184. doi: 10.1016/j.anifeedsci.2007.10.016.

Boerjan, W., Ralph, J. and Baucher, M. (2003) 'Lignin biosynthesis.', *Annu Rev Plant Biol*, 54, pp. 519–46. doi: 10.1146/annurev.arplant.54.031902.134938.

Boldizar, A. *et al.* (1987) 'Prehydrolyzed cellulose as reinforcing filler for thermoplastics.', *Intern. J. Polymeric Mater.*, 11, pp. 229–262. doi: https://doi.org/10.1080/00914038708078665.

Börjesson, M. and Westman, G. (2015) *Crystalline Nanocellulose — Preparation ,*

Modification , and Properties. doi: 10.5772/61899.

Boufi, S. *et al.* (2016) 'Nanofibrillated cellulose as an additive in papermaking process: A review', *Carbohydr Polym.*, 154, pp. 151–166. doi: https://doi.org/10.1016/j.carbpol.2016.07.117.

Bruijnincx, P. C. A., Rinaldi, R. and Weckhuysen, B. M. (2015) 'Unlocking the potential of a sleeping giant: lignins as sustainable raw materials for renewable fuels, chemicals and materials', *Green Chemistry*. Royal Society of Chemistry, pp. 4860–4861. doi: 10.1039/c5gc90055g.

Capecchi, E. *et al.* (2019) 'Enzyme-Lignin Nanocapsules Are Sustainable Catalysts and Vehicles for the Preparation of Unique Polyvalent Bioinks', *Biomacromolecules*, 20(5), pp. 1975–1988. doi: 10.1021/acs.biomac.9b00198.

Cassie, B. D. and Baxter, S. (1944) 'WETTABILITY OF POROUS SURFACES', *Royal Society of Chemistry*, 40(5), pp. 546–551.

Chakar, F. S. and Ragauskas, A. J. (2004) 'Review of current and future softwood kraft lignin process chemistry', *Industrial Crops & Products*, 20, pp. 131–141. doi: 10.1016/j.indcrop.2004.04.016.

Chen, N., Dempere, L. A. and Tong, Z. (2016) 'Synthesis of pH-Responsive Lignin-Based Nanocapsules for Controlled Release of Hydrophobic Molecules. ACS Sustain. Chem. Eng.4, 5204–5211.', *ACS Sustainable Chem*, 4(10), pp. 5204–5211. doi: 10.1021/acssuschemeng.6b01209.

Crestini, C. *et al.* (2017) 'On the structure of softwood kraft lignin', *Green Chemistry*. Royal Society of Chemistry, pp. 4104–4121. doi: 10.1039/c7gc01812f.

Dai, L. *et al.* (2017) 'Lignin Nanoparticle as a Novel Green Carrier for the Efficient Delivery of Resveratrol.', *ACS Sustain. Chem.*, pp. 8241–8249. doi: 10.1021/acssuschemeng.7b01903.

Dimmel, D. R. (2010) 'Overview. In: Lignin and Lignans: Advances in Chemistry, C. Heitner, D.R. Dimmel, J.A. Schmidt (eds.), CRC Press, Boca Raton, FL, USA, pp. 1–10.'

Dorrestijn, E. *et al.* (2000) 'The occurrence and reactivity of phenoxyl linkages in lignin and low rank coal.', *Analytical and Applied Pyrolysis*, 54, pp. 153–92. doi: https://doi.org/10.1016/S0165-2370(99)00082-0.

Dufresne, A. (2012) *Nanocellulose*. Berlin/Boston.: Walter de Gruyter GmbH. doi: http://dnb.d-nb.de.

Dufresne, A. (2013) 'Nanocellulose: A new ageless bionanomaterial', *Materials Today*, 16(6), pp. 220–227. doi: 10.1016/j.mattod.2013.06.004.

Dumanli, A. G. (2017) 'Nanocellulose and its Composites for Biomedical Applications', *Curr Med Chem.*, 24, pp. 512–528. doi: 10.2174/0929867323666161014124008.

Eyley, S. and Thielemans, W. (2014) 'Surface modification of cellulose nanocrystals', pp. 7764–7779. doi: 10.1039/c4nr01756k.

Farooq, M. *et al.* (2019) 'Strong, Ductile, and Waterproof Cellulose Nano fi bril Composite Films with Colloidal Lignin Particles', *Biomacromolecules*, 20(2), pp. 693–704. doi: 10.1021/acs.biomac.8b01364.

Fengel, D. and Wegener, G. (1984) 'Wood—chemistry, ultrastructure, reactions', p. 613. doi: https://doi.org/10.1002/pol.1985.130231112.

Figueiredo, P. *et al.* (2017) 'In vitro evaluation of biodegradable lignin-based nanoparticles for drug delivery and enhanced antiproliferation effect in cancer cells.', *Biomaterials*, 121, pp. 97–108. doi: https://doi.org/10.1016/j.biomaterials.2016.12.034.

De France, K. J., Hoare, T. and Cranston, E. D. (2017) 'Review of Hydrogels and Aerogels Containing Nanocellulose Chem Mater', 29, pp. 4609–4631. doi: 10.1021/acs.chemmater.7b00531.

Frangville, C. (2012) 'Fabrication of Environmentally Biodegradable Lignin Nanoparticles', *Chemphyschem*, 27695, pp. 4235–4243. doi: 10.1002/cphc.201200537.

Gellerstedt, G. (2015) 'Softwood kraft lignin : Raw material for the future', *Industrial Crops & Products*. Elsevier B.V., 77, pp. 845–854. doi: 10.1016/j.indcrop.2015.09.040.

Gîlcă, I.-A. and Popa, V. I. (2013) 'Study on Biocidal Properties of Some Nanoparticles Based on Epoxy Lignin.', *Cellul. Chem. Technol.*, 47, pp. 3–4.

Gilca, I. A., Popa, V. I. and Crestini, C. (2015) 'Ultrasonics Sonochemistry Obtaining lignin nanoparticles by sonication', *Ultrasonics - Sonochemistry*. Elsevier B.V., 23, pp. 369–375. doi: 10.1016/j.ultsonch.2014.08.021.

Gonugunta, P. *et al.* (2012) 'A Study on Synthesis and Characterization of Biobased Carbon Nanoparticles from Lignin', *World Journal of Nano Science and Engineering*, 2012(September), pp. 148–153. doi: 10.4236/wjnse.2012.23019.

Habibi, Y. *et al.* (2008) 'Bionanocomposites based on poly(ε-caprolactone)-grafted cellulose nanocrystals by ring-opening polymerization', *Journal of Materials Chemistry*, pp. 5002–5010. doi: 10.1039/B809212E.

Hayashi, T., Marsden, M. P. F. and Delmer, D. P. (1987) 'Pea Xyloglucan and Cellulose VI. Xyloglucan-Cellulose Interactions in Vitro and in Vivo', *plant Physiology*, pp. 384–389. doi: https://doi.org/10.1104/pp.83.2.384.

Henriksson, M. *et al.* (2007) 'An environmentally friendly method for enzyme-assisted preparation of microfibrillated cellulose (MFC) nanofibers', *ScienceDirect*, 43, pp. 3434–3441. doi: 10.1016/j.eurpolymj.2007.05.038.

Herrera, M. *et al.* (2018) 'Preparation and evaluation of high-lignin content cellulose nanofibrils from eucalyptus pulp', *Cellulose*, 25(5), pp. 3121–3133. doi: 10.1007/s10570-018-1764-9.

Herrick, F. W. *et al.* (1983) 'Microfibrillated cellulose: morphology and accessibility'.

Hirota, M. *et al.* (2010) 'Water dispersion of cellulose II nanocrystals prepared by TEMPO-mediated oxidation of mercerized cellulose', *Springer Science+Business Media*, pp. 279–288. doi: 10.1007/s10570-009-9381-2.

Hortling, B., Turunen, E. and Kokkonen, P. (1999) 'Procedure for molar mass distribution measurements of lignins of different origin. In: Proceedings of the 10th international symposium on wood and pulping chemistry, Yokohama, Japan, 7 – 10 June 1999, vol 1, p48'.

Houtman, C. J. and Atalla, R. H. (1995) 'Cellulose-Lignin Interactions (A Computational Study)', *Plant Physiology*, pp. 977–984. doi: https://doi.org/10.1104/pp.107.3.977.

Hu, S. *et al.* (2014) 'High energy density supercapacitors from lignin derived submicron activated carbon fibers in aqueous electrolytes.', *J. Power Sources*, 270, pp. 106–112. doi: https://doi.org/10.1016/j.jpowsour.2014.07.063.

Iiyama, K., Lam, T. B. T. and Stone, B. A. (1994) 'Covalent cross-links in the cell wall.', *Plant Physiology*, 104(2), pp. 315–320.

J. Loos, P. C. Thüne, J. W. Niemantsverdriet, and P. J. L. (1999) 'Polymerization and Crystallization of Polyethylene on a Flat Model Catalyst Macromolecules', *Macromolecules*, 32, pp. 8910–8. doi: 10.1021/ma990891z.

J.L., W., Bédué, O. and Mercier, J. P. (2010) *Cellulose Science and Technology*. 1st edn.

Jiang, C. *et al.* (2010) 'A new and sensitive catalytic resonance scattering spectral assay for the detection of laccase using guaiacol as substrate', *Luminescence*, pp. 500–505. doi: 10.1002/bio.1259.

Jonas, R. and Farah, L. F. (1998) 'Production and application of microbial cellulose', *Polymer Degradation and Stabiity*, 3910(97), pp. 101–106. doi: https://doi.org/10.1016/S0141-3910(97)00197-3.

Kai, D. *et al.* (2016) 'Towards lignin-based functional materials in a', *Green Chemistry*. Royal Society of Chemistry, 18, pp. 1175–1200. doi: 10.1039/c5gc02616d.

Kangas, H. *et al.* (2016) 'High-consistency enzymatic fibrillation (HefCel) – a cost-efficient way to produce cellulose nanofibrils (CNF)', *Advanced Materials*, pp. 181–183.

Kaushik, M. and Moores, A. (2016) 'Review: nanocelluloses as versatile supports for metal nanoparticles and their applications in catalysis', *Green Chem*, 18, pp. 622–637. doi: 10.1039/C5GC02500A.

Klemm, D. *et al.* (2001) 'Bacterial synthesized cellulose — artificial blood vessels for microsurgery.', *Prog. Polym. Sci.*, 26, pp. 1561–1603. doi: https://doi.org/10.1016/S0079-6700(01)00021-1.

Klemm, D. *et al.* (2005) 'Cellulose: Fascinating biopolymer and sustainable raw material', *Angewandte Chemie - International Edition*, 44(22), pp. 3358–3393. doi: 10.1002/anie.200460587.

Klemm, D. *et al.* (2011) 'Nanocelluloses: A New Family of Nature-Based Materials', *Green Nanomaterials*, 50, pp. 5438–5466. doi: 10.1002/anie.201001273.

Kontturi, E. (2011) 'UPM-KYMMENE CORPORATION. Patent WO2011/114005'.

Lai, C. *et al.* (2014) 'Free-standing and mechanically flexible mats consisting of electrospun carbon nanofibers made from a natural product of alkali lignin as binder-free electrodes for high-performance supercapacitors. J. Power Sources 247, 134–141.'

Laurichesse, S. and Avérous, L. (2014) 'Progress in Polymer Science Chemical modification of lignins : Towards biobased polymers', *Progress in Polymer Science*, 39(7), pp. 1266–1290. doi: 10.1016/j.progpolymsci.2013.11.004.

Lavoine, N. *et al.* (2012) 'Microfibrillated cellulose - Its barrier properties and applications in cellulosic materials: A review', *Carbohydrate Polymers*, 90(2), pp. 735–764. doi: 10.1016/j.carbpol.2012.05.026.

Lawoko, M. and Henriksson, G. (2005) 'Structural Differences between the Lignin - Carbohydrate Complexes Present in Wood and in Chemical Pulps', *Biomacromolecules*, 6, pp. 3467–3473. doi: 10.1021/bm058014q.

Lian, Y. *et al.* (2018) 'Preparation of Hemicellulose-based Hydrogel and its Application as an Adsorbent Towards Heavy Metal Ions', *Bioresources*, 13(2), pp. 3208–3218.

Lievonen, M. *et al.* (2016) 'A simple process for lignin nanoparticle preparation', *Green Chemistry*, 18(5), pp. 1416–1422. doi: 10.1039/c5gc01436k.

Liu, Y. (2018) 'Strong and Flexible Nanocomposites of Carboxylated Cellulose Nano fi bril Dispersed by Industrial Lignin', *Sustainable Chemistry and Engineering*, 6, pp. 5524–5532. doi: 10.1021/acssuschemeng.8b00402.

Lu, Q. *et al.* (2012) 'Comparative antioxidant activity of nanoscale lignin prepared by a supercritical antisolvent (SAS) process with non-nanoscale lignin.', *Food Chem.*, 135, pp. 63–67. doi: https://doi.org/10.1016/j.foodchem.2012.04.070.

Lucenius, J., Parikka, K. and Österberg, M. (2014) 'Nanocomposite films based on cellulose nanofibrils and water-soluble polysaccharides', *Reactive and Functional Polymers*, 85, pp. 167–174. doi: 10.1016/j.reactfunctpolym.2014.08.001.

Malainine, M. E. *et al.* (2003) 'Structure and morphology of cladodes and spines of Opuntia ficus-indica. Cellulose extraction and charac- terisation.', *Carbohydr. Polym.*, 51, p. 77–83. doi: 10.1016/S0144-8617(02)00157-1.

Man, Z. *et al.* (2011) 'Preparation of Cellulose Nanocrystals Using an Ionic', *Polymers and the Environment*, 19, pp. 726–731. doi: 10.1007/s10924-011-0323-3.

Moon, R. J. *et al.* (2011) 'Chem Soc Rev', *Chem. Soc. Rev*, 40, pp. 3941–3994. doi: 10.1039/c0cs00108b.

Mousa, M. H., Dong, Y. and Davies, I. J. (2016) 'Recent advances in bionanocomposites: Preparation, properties, and applications', *Int J Polym Mater Polym Biomater*, 65, pp. 225–254. doi: https://doi.org/10.1080/00914037.2015.1103240.

Nevárez, L. A. M. *et al.* (2011) 'Biopolymer-based nanocomposites: Effect of lignin acetylation in cellulose triacetate films.', *Sci. Technol. Adv. Mater.*, 12., p. 45006.

Nishimura, H. *et al.* (2018) 'Direct evidence for α ether linkage between lignin and carbohydrates in wood cell walls', *Scientific Reports*, 8(March), pp. 1–11. doi: 10.1038/s41598-018-24328-9.

Nishiyama, Y. *et al.* (2003) 'Periodic Disorder along Ramie Cellulose Microfibrils', *Biomacromolecules*, 4, pp. 1013–1017. doi: 10.1021/bm025772x.

Nypelö, T. E., Carrillo, C. A. and Rojas, O. J. (2015) 'Lignin supracolloids synthesized from (W/O) microemulsions: Use in the interfacial stabilization of Pickering systems and organic carriers for silver metal.', *Soft Matter*, 11, pp. 2046–2054. doi: 10.1039/c4sm02851a.

Okita, Y. *et al.* (2011) 'TEMPO-Oxidized Cellulose Nanofibrils Dispersed in Organic Solvents', *Biomacromolecules*, 12, pp. 518–522. doi: 10.1021/bm101255x.

Osong, S. H., Norgren, S. and Engstrand, P. (2016) 'Processing of wood-based microfibrillated cellulose and nanofibrillated cellulose, and applications relating to papermaking: a review Cellulose', 23, pp. 93–123.

Österberg, M. *et al.* (2013) 'A fast method to produce strong NFC films as a platform for barrier and functional materials', *ACS Applied Materials and Interfaces*, 5(11), pp. 4640–4647. doi: 10.1021/am401046x.

Pääkkö, M. *et al.* (2007) 'Enzymatic Hydrolysis Combined with Mechanical Shearing and High-Pressure Homogenization for Nanoscale Cellulose Fibrils and Strong Gels', *Biomacromolecules*, 9, pp. 1934–1941. doi: 10.1021/bm061215p.

Popa, V. I. *et al.* (2011) 'Nanoparticles based on modified lignins with biocide properties.', *Cellul. Chem. Technol.*, 45, p. 221–226.

Qian, Y., Zhang, Q., *et al.* (2014) 'CO2-responsive diethylaminoethyl-modified lignin nanoparticles and their application as surfactants for CO2/N2-switchable Pickering emulsions', *Green Chemistry*, 16, pp. 4963–4968. doi: 10.1039/c4gc01242a.

Qian, Y., Deng, Y., *et al.* (2014) 'Formation of uniform colloidal spheres from lignin, a renewable resource recovered from pulping spent liquor', *Green Chemistry*, 16, pp. 2156–2163. doi: 10.1039/c3gc42131g.

Qian, Y. *et al.* (2017) 'Fabrication of uniform lignin colloidal spheres for developing natural broad-spectrum sunscreens with high sun protection factor.', *Ind. Crops*

Prod., 101, p. 54–60. doi: https://doi.org/10.1016/j.indcrop.2017.03.001.

Quellmalz, A. and Mihranyan, A. (2015) 'Citric Acid Cross-Linked Nanocellulose-Based Paper for Size- Exclusion Nano fi ltration', *ACS Biomater. Sci. Eng*, 1, pp. 271–276. doi: 10.1021/ab500161x.

Rajwade, J. M., Paknikar, K. M. and Kumbhar, J. V (2015) 'Applications of bacterial cellulose and its composites in biomedicine', *Appl Microbiol Biotechnol*, 99, pp. 2491–2511. doi: 10.1007/s00253-015-6426-3.

Ralph, J. *et al.* (2009) 'Quinone methides in lignification', in Rokita, S. E. (ed.) *Quinone Methides*, pp. 385–420. doi: https://doi.org/10.1002/9780470452882.ch12.

Rånby, B. G. (1949) 'Aqueous Colloidal Solutions of Cellulose Micelles.' Uppsala, pp. 649–650. doi: 10.3891/acta.chem.scand.03-0649.

Rojo, E. *et al.* (2015) 'Comprehensive elucidation of the effect of residual lignin on the physical, barrier, mechanical and surface properties of nanocellulose film', *Green Chemistry*. Royal Society of Chemistry, 17, pp. 1853–1866. doi: 10.1039/c4gc02398f.

Rosenau, T., Antje, P. and Hell, J. (eds) (2019) *Cellulose Science and Technology: Chemistry, Analysis, and Applications*.

Roy, D. *et al.* (2009) 'Cellulose modification by polymer grafting : a review', *Chemical Society Reviews*, 38(7). doi: 10.1039/b808639g.

Sarkanen, K. and Ludwig, C. (1971) 'Lignins: occurrence, formation, structure and reactions. New York: Wiley-Interscience; 916 pp.', *Progress in Polymer Science*, (39), pp. 1266–1290. doi: https://doi.org/10.1016/j.progpolymsci.2013.11.004.

Scheller, H. V. and Ulvskov, P. (2010) 'Hemicelluloses', *The Annual Review ofPlant Biology*, 61, pp. 263–89. doi: 10.1146/annurev-arplant-042809-112315.

Schlesing, W., Buhk, M. and Osterhold, M. (2004) 'Dynamic mechanical analysis in coatings industry.', *Prog Org Coat*, 49, pp. 197–208. doi: https://doi.org/10.1016/j.porgcoat.2003.09.009.

Sharma, A. *et al.* (2019) 'Commercial Application of Cellulose Nano-composites - A review', *Biotechnology Reports*. doi: https://doi.org/10.1016/j.btre.2019.e00316.

Shoda, M. and Sugano, Y. (2005) 'Recent Advances in Bacterial Cellulose Production', *Biotechnology and Bioproccess ENgineering*, 10(1), pp. 1–8. doi: https://doi.org/10.1007/BF02931175.

Silva, C. G. *et al.* (2013) 'Adding value to lignins isolated from sugarcane bagasse and Miscanthus', *IndustIrial Crops & Products*, 42, pp. 87–95. doi: 10.1016/j.indcrop.2012.04.040.

Sipponen, M. H., Smyth, M., *et al.* (2017) 'All-lignin approach to prepare cationic colloidal lignin particles: Stabilization of durable Pickering emulsions', *Green Chemistry*, 19(24), pp. 5831–5840. doi: 10.1039/c7gc02900d.

Sipponen, M. H., Rahikainen, J., *et al.* (2017) 'Structural changes of lignin in biorefinery pretreatments and consequences to enzyme-lignin interactions', *Nordic Pulp and Papers Research*, 32(4), pp. 547–568. doi: 10.3183/npprj-2017-32-04_p550-571_sipponen.

Sipponen, M. H. *et al.* (2018) 'Spatially confined lignin nanospheres for biocatalytic ester synthesis in aqueous media', *Nature Communications*. Springer US, 9(1), pp. 1–7. doi: 10.1038/s41467-018-04715-6.

Sipponen, M. H. *et al.* (2018) 'Understanding Lignin Aggregation Processes. A Case Study: Budesonide Entrapment and Stimuli Controlled Release from Lignin Nanoparticles', *ACS Sustainable Chemistry and Engineering*. American Chemical Society, 6(7), pp. 9342–9351. doi: 10.1021/acssuschemeng.8b01652.

Siqueira, G. and Abdillahi, H. (2010) 'High reinforcing capability cellulose nanocrystals extracted from Syngonanthus nitens (Capim Dourado)', *Cellulose*, 17, pp. 289–298. doi: 10.1007/s10570-009-9384-z.

Siquieira, G. *et al.* (2010) 'Morphological investigation of nanoparticles obtained from combined mechanical shearing , and enzymatic and acid hydrolysis of sisal fibers',

Cellulose, 17, pp. 1147–1158. doi: 10.1007/s10570-010-9449-z.

Siró, I. and Plackett, D. (2010) 'Microfibrillated cellulose and new nanocomposite materials: a review Cellulose, 17 pp. 459-494'.

Smolarski, N. (2012) *High-value opportunities for lignin: unlocking its potential. Paris: Frost & Sullivan*.

Stenius, P. (2000) *Forest Products Chemistry. Papermaking Science and Technology. Fapet Oy: Helsinki.* Stenius, P. Edited by P. S. Johan Gullichsen, Hannu Paulapuro. Helsinki.

Sulaeva, I. *et al.* (2015) 'Bacterial cellulose as a material for wound treatment : Properties and modi fi cations . A review', *Biotechnology Advances*, 33(8), pp. 1547–1571. doi: 10.1016/j.biotechadv.2015.07.009.

Tomani, P. (2010) 'The lignoboost process', *Cellulose Chemistry and Technology*, 44(1–3), pp. 53–58.

Tortora, M. *et al.* (2014) 'Ultrasound Driven Assembly of Lignin into Microcapsules for Storage and Delivery of Hydrophobic Molecules.', *Biomacromolecules*, 15, p. 1634–1643. doi: 10.1021/bm500015j.

Ul-islam, M., Khan, S. and Khattak, W. A. (2015) 'Synthesis , Chemistry , and Medical Application of Bacterial Cellulose Synthesis , Chemistry , and Medical Application of Bacterial Cellulose Nanocomposites', *Advanced Structured Materials*, 74. doi: 10.1007/978-81-322-2473-0.

UPM (2011) *Metsiemme puita - Träden i våra skoga*. Available at: https://www.upmmetsa.fi/siteassets/yhteiset/pdft/julisteet/metsiemme-puita-upm-juliste.pdf?_t_id=1B2M2Y8AsgTpgAmY7PhCfg%3D%3D&_t_q=mänty&_t_tags=language:fi%2Csiteid:dc93f855-8b24-44df-9d50-7cd07e3cad27&_t_ip=130.233.92.134&_t_hit.id=Solita_Epi_Web_Business_ContentTypes_Files_GenericFile/_558871f2-7b2e-43a9-8a1e-03736f22b377&_t_hit.pos=4

(Accessed: 16 April 2019).

Vanholme, R. *et al.* (2010) 'Lignin Biosynthesis and Structure', *Plant Physiology*, 153, pp. 895–905. doi: 10.1104/pp.110.155119.

Wågberg, L. *et al.* (2008) 'The build-up of polyelectrolyte multilayers of microfibrillated cellulose and cationic polyelectrolytes.', *Langmuir*, 24, p. 784–795. doi: 10.1021/la702481v.

Wang, Q. *et al.* (2018) 'Flexible cellulose nanopaper with high wet tensile strength, high toughness and tunable ultraviolet blocking ability fabricated from tobacco stalk via a sustainable method', *J. Mater. Chem. A*, 6, pp. 13021–13030. doi: 10.1039/c8ta01986j.

Xue, Y., Mou, Z. and Xiao, H. (2017) 'Nanocellulose as a sustainable biomass material: structure, properties, present status and future prospects in biomedical applications Nanoscale', *Nanoscale*, 9, pp. 14758–14781. doi: 10.1039/C7NR04994C.

Yearla, S. R. and Padmasree, K. (2016) 'Preparation and characterisation of lignin nanoparticles: Evaluation of their potential as antioxidants and UV protectants. J. Exp. Nanosci.11, 289–302.', *Journal of Experimental Nanoscience*, 11(4), pp. 289–302. doi: http://dx.doi.org/10.1080/17458080.2015.1055842.

Yiamsawas, D. *et al.* (2014) 'Biodegradable lignin nanocontainers.', *RSC Adv*, 4, p. 11661. doi: 10.1039/C3RA47971D.

Yiamsawas, D. *et al.* (2017) 'Morphology-Controlled Synthesis of Lignin Nanocarriers for Drug Delivery and Carbon Materials.', *ACS Biomater. Sci. Eng.*, 3, p. 2375–2383. doi: 10.1021/acsbiomaterials.7b00278.

Zimniewska, M., Kozłowski, R. and Batog, J. N. (2008) 'Modified Linen Fabric as a Multifunctional Product.', *Mol. Cryst. Liq. Cryst.*, 484, p. 43/(409)–50/(416). doi: 10.1080/15421400801903395.

12. Appendix

1. Nanocomposite films displaying irregular morphology due to foaming: a) 5CLP-HefCel b) 25CLP-HefCel c) LigHefCel-10CLP-1000LAC

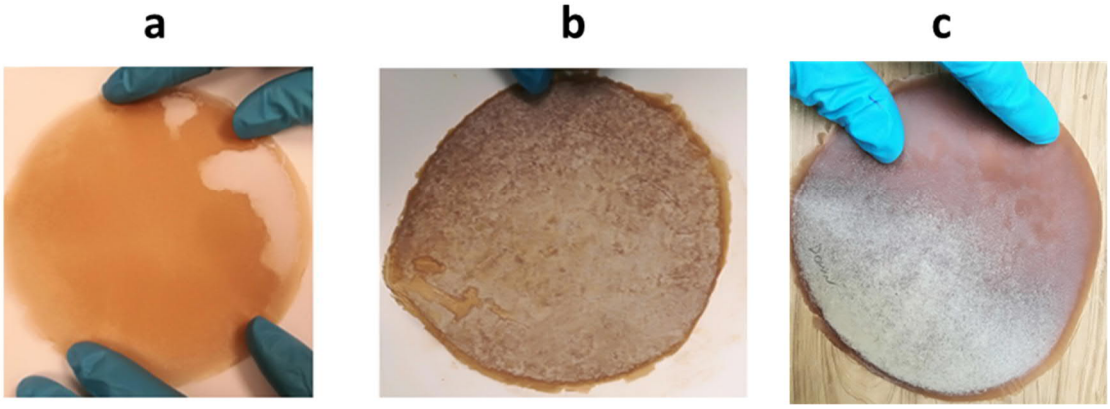

2. ANOVA analysis on Young's modulus of laccase experiment

One-Way AOV for: LigHefCel, LigHefCel-10CLP, LigHefCel-500LAC, LigHefCel-10CLP-50LAC, LigHefCel-10CLP-500LAC, LigHefCel-10CLP-5000LAC

Source	df	Sum of Square	MS	F	Significance level P
Between	5	1494.67	298.934	2.88	0.0238
Within	48	4988.5	103.927		
Total	53	6483.17			

Statistix 9.0 3/7/2019, 6:45:07 PM

Tukey HSD All-Pairwise Comparisons Test

Variable	Mean	Homogeneous Groups
LigHefCel-10CLP-50LAC	89.294	A
LigHefCel-10CLP-500LAC	81.977	A
LigHefCel-10CLP	80.44	A
LigHefCel	75.718	A
LigHefCel-10CLP-5000LAC	74.872	A
LigHefCel-500LAC	72.823	A

Alpha 0.01 Standard Error for Comparison 4.4543 TO 5.2761

Critical Q Value 5.047 Critical Value for Comparison 15.897 TO 18.830

There are no significant pairwise differences among the means.

3. Water contact angle:

One-Way AOV for: LigHefCel, LigHefCel-10CLP, LigHefCel-500LAC, LigHefCel-10CLP-50LAC, LigHefCel-10CLP-500LAC, LigHefCel-10CLP-5000LAC

Source	df	Sum of Square	MS	F	Significance level P
Between	5	1260.73	252.145	9.5	0.0007
Within	12	318.56	26.547		
Total	17	1579.29			

Tukey HSD All-Pairwise Comparisons Test

Variable	Mean	Homogeneous Groups
LHC10500	58.885	A
LHC105000	53.598	AB
LigHC500L	47.914	ABC
LHC1050	42.05	ABC
LigHefCel	38.026	BC
LigHC10CL	35.34	C

Alpha 0.01 Standard Error for Comparison 4.2069

Critical Q Value 6.103 Critical Value for Comparison 18.156

There are 3 groups (A, B, etc.) in which the means are not significantly different from one another.

4. Water contact angle results

Pressurized filter	**Down**			**UP**			**Mean**	
Sample	**Mean**	**SD**	**SD/2**	**Mean**	**SD**	**SD/2**	**Mean (Down,UP)**	**SD/2 Mean**
HefCel	19.40	7.65	3.83	37.60	5.72	2.86	**28.50**	**3.34**
1CLP	19.10	5.15	2.57	37.63	3.71	1.85	**28.37**	**2.21**
5CLP	34.32	3.29	1.64	36.56	3.28	1.64	**35.44**	**1.64**
10CLP	25.00	3.59	1.79	36.20	3.54	1.77	**30.60**	**1.78**
15CLP	22.59	2.75	1.38	30.57	4.32	2.16	**26.58**	**1.77**
25CLP	21.62	7.39	3.69	36.77	4.88	2.44	**29.19**	**3.07**

Ambient dry	Down			UP			MEAN	
Sample	Mean	SD	SD/2	Mean	SD	SD/2	Mean (Down,UP)	SD/2 mean
HefCel	47.25	1.03	0.51	52.82	1.97	0.98	**50.04**	**0.75**
1CLP	36.40	2.16	1.08	57.10	3.05	1.53	**46.75**	**1.30**
5CLP	35.33	5.36	2.68	68.74	2.67	1.33	**52.04**	**2.01**
10CLP	39.44	2.86	1.43	53.86	4.60	2.30	**46.65**	**1.87**
15CLP	25.91	1.27	0.63	55.84	6.03	3.02	**40.88**	**1.82**
25CLP	30.11	3.49	1.75	53.29	2.89	1.45	**41.70**	**1.60**

Laccase experiment	Down			UP			MEAN	
Sample	Mean	SD	SD/2	Mean	SD	SD/2	CA mean (Down,UP)	SD/2 mean
LigHefCel	32.99	5.18	2.59	40.47	6.48	3.24	**36.73**	**2.91**
LigHefCel-10CLP	35.32	2.38	1.19	33.58	8.80	4.40	**34.45**	**2.80**
LigHefCel-500LAC	47.59	11.30	5.65	49.77	6.15	3.07	**48.68**	**4.36**
LigHefCel-10CLP-50LAC	40.94	3.66	1.83	42.98	3.61	1.81	**41.96**	**1.82**
LigHefCel-10CLP-500LAC	55.01	1.80	0.90	62.10	4.84	2.42	**58.56**	**1.66**
LigHefCel-10CLP-1000LAC	36.40	6.11	3.06	70.04	3.26	1.63	**53.22**	**2.34**
LigHefCel-10CLP-5000LAC	41.24	7.54	3.77	64.55	1.53	0.76	**52.90**	**2.27**

5. Nanocellulose composites which were treated with laccase displayed reddish color. a) LigHefCel b) LigHefCel-10CLP c) LigHefCel-10CLP-50LAC d) LigHefCel-10CLP-500LAC e) LigHefCel-10CLP-5000LAC